MODALITIES OF CHOLESTEROL BINDING AND MODULATION OF THE NPC PROTEINS AND SCAP

APPROVED BY COMMITTEE

Michael S. Brown, M.D. (Mentor) _____

Joseph L. Goldstein, M.D. (Mentor) _____

Russell Debose-Boyd, Ph.D. (Chair) _____

Richard Auchus, M.D., Ph.D. _____

Jef DeBrabander, Ph.D. _____

DEDICATION

This is dedicated to my wife, Amy, and daughter, Yael.

MODALITIES OF CHOLESTEROL BINDING AND MODULATION OF THE NPC PROTEINS AND SCAP

by

MASSOUD MOTAMED

DISSERTATION

Presented to the Faculty of the Graduate School of Biomedical Sciences

The University of Texas Southwestern Medical Center at Dallas

In Partial Fulfillment of the Requirements

For the Degree of

DOCTOR OF PHILOSOPHY

The University of Texas Southwestern Medical Center at Dallas

Dallas, Texas

June, 2011

MODALITIES OF CHOLESTEROL BINDING AND MODULATION OF THE NPC PROTEINS AND SCAP

Publication No:_____

Massoud Motamed, Ph.D.

The University of Texas Southwestern Medical Center at Dallas, 2011

Supervising Professors: Michael S. Brown, M.D. and Joseph L. Goldstein, M.D.

Low density lipoproteins (LDL) and related plasma lipoproteins deliver cholesterol to cells by receptor-mediated endocytosis. The lipoprotein is degraded in late endosomes and lysosomes, allowing cholesterol to be released. Export of cholesterol from late endosomes and lysosomes (hereafter referred to as lysosomes) requires two lysosomal proteins: Niemann-Pick C2 (NPC2), a soluble protein of 132 amino acids; and NPC1, a membrane protein with 13 putative membrane-spanning helices. Recessive loss-of-function mutations in either NPC2 or NPC1 produce NPC disease, which causes death owing to lipid accumulation in lysosomes of liver, brain, and lung.

Consistent with their cholesterol export role, NPC2 and NPC1 both bind to cholesterol. The cholesterol binding site on NPC1 is located in the NH_2-terminal domain (NTD), which projects into the lysosomal lumen. This domain, designated NPC1 (NTD), can be expressed *in vitro* as a soluble protein of 240 amino acids that maintains cholesterol binding activity. This thesis studies NPC2 in detail as summarized below.

Despite a shared role as cholesterol binding proteins, NPC2 and NPC1 (NTD) bind to cholesterol in opposite orientations. The crystal structures of NPC2 and NPC1 (NTD) have been solved, and NPC2 binds cholesterol with the iso-octyl chain facing the interior of the protein, whereas, NPC1(NTD) binds cholesterol with the 3ß-hydroxyl facing the interior of the protein. Another striking difference is the kinetics of this cholesterol binding. NPC2 binds and releases cholesterol rapidly (half-time < 2 min at 4^oC), while NPC1 (NTD) binds cholesterol very slowly (half-time > 2 hr at 4^oC). However, NPC2 can stimulate the rate of cholesterol binding to NPC1 (NTD) (>15-fold *in vitro*). This stimulation of cholesterol binding to NPC1 (NTD) by NPC2 is believed to occur through a direct transfer of cholesterol from NPC2 to NPC1(NTD).

Amino acid residues important for binding or transfer of cholesterol on NPC2 were identified through alanine scan mutagenesis. Residues that decreased binding thermodynamics and/or kinetics mapped to areas surrounding the binding pockets on the crystal structures; residues that decreased transfer, but not binding, mapped to discrete surface patches near the exposed residues of the binding pockets. These surface patches may be sites where the two proteins interact to transfer cholesterol. The most deleterious binding mutant was P120S, a residue in the cholesterol binding pocket; the most deleterious transfer mutant was V81D, a residue on the hydrophobic patch extending outward from the cholesterol binding pocket. The

above mutants of NPC2 were unable to rescue LDL-stimulated cholesteryl ester synthesis in NPC2-deficient cells, in contrast to wild-type NPC2.

Once LDL-derived cholesterol leaves the lysosomes, it is transported to the endoplasmic reticulum (ER), where it serves a regulatory role in cholesterol homeostasis. In the ER, these regulatory functions include activation of acetyl-coenzyme A acetyltransferase (ACAT), allowing for esterification of cholesterol for storage, and regulation of sterol regulatory element–binding protein (SREBP) localization, a transcription factor that regulates key enzymes for cholesterol synthesis.

SREBP cleavage-activating protein (Scap) is the switch that controls SREBP, and therefore cholesterol synthesis. Scap senses cholesterol abundance in the ER and acts as an escort protein. In sterol depleted cells, Scap escorts SREBP to the Golgi complex, where two proteases cleave SREBP, thereby releasing its transcriptionally active domain so that it can go to the nucleus and activate transcription of genes involved in cholesterol synthesis and uptake. When cholesterol in abundant, the sterol binds to Scap and triggers a conformational change in the protein that prevents it from escorting SREBPs to the Golgi for proteolytic cleavage.

Scap is a 1276 amino acid protein that consists of two domains: an N-terminal domain with 8 transmembrane spanning regions and a C-terminal domain that projects into the cytosol and associates with SREBPs. Previous studies have localized the cholesterol-binding activity of Scap to its membrane domain. Studies described in this thesis identify the cholesterol binding pocket in Scap and identify key residues that play an important role in the protein's responsiveness to cholesterol binding.

The first loop region of Scap (hereafter referred to as Scap(Loop1)) was purified as a recombinant protein and found to have cholesterol binding activity. The specificity of this sterol

binding was determined through competition studies and shown to be physiologically relevant. Additionally, this binding affinity and specificity was similar to that of the membrane domain of Scap. Subsequently, alanine scan mutagenesis was performed on Scap(Loop1). Through this approach, several mutations of Scap were identified that constitutively adopt the cholesterol-bound state. This data demonstrates that Scap(Loop1) binds to cholesterol and that the binding then helps induce the conformational change required for Scap to anchor SREBP in ER membranes.

ACKNOWLEDGEMENTS

I thank Dr. Michael Brown and Dr. Joseph Goldstein, for the opportunity to learn biology. Coming from an organic chemistry background, biology required a huge adjustment, and they have been patient and supportive the whole way. I have a better understanding of what science is and how to design an interpretable experiment.

I also thank my thesis committee members Drs. Russell DeBose-Boyd, Richard Auchus, and Jef DeBrabander for constant encouragement and ideas.

I would like to acknowledge members of the Brown and Goldstein group who have invested time to teach me science- Rodney Infante, Michael Wang, Lina Abi-Mosleh, and Akash Das. Michael Wang was of great guidance and taught me how to make progress. Additionally, I would like to thank Yinxin Zhang and Dorothy Williams for helping me through experiments and keeping a positive attitude no matter how daunting the work load was.

My family has been a great encouragement throughout my education. My parents and wife have understood the importance of the time and preoccupation I have invested in the lab. My wife and daughter have provided me with a great source of joy, even when science isn't working the way it "should."

TABLE OF CONTENTS

PRIOR PUBLICATIONS

Motamed M, Bunnelle EM, Singaram SW. Sarpong R. Pt(II)-Catalyzed Synthesis of 1,2-Dihydropyridines from Aziridinyl Propargylic Esters. Org Lett. 2007 May 24:9(11):2167-70.

Wang ML, **Motamed M**, Infante RE, Abi-Mosleh L, Kwon HJ, Brown MS, Goldstein JL. Identification of Surface Residues on Niemann-Pick C2 (NPC2) Essential for Hydrophobic Handoff of Cholesterol to NPC1 in Lysosomes. Cell Metab. 2010 Aug 4;12(2):166-73.

Motamed M, Zhang Y, Wang ML, Seemann J, Kwon HJ, Goldstein JL, Brown MS. Identification of Luminal Loop 1 of Scap as the Sterol Sensor that Maintains Cholesterol Homeostasis. J Biol Chem. 2011 May 20;286(20):18002-12.

LIST OF FIGURES

CHAPTER 1

CHAPTER 2

CHAPTER 3

LIST OF ABBREVIATIONS

ACAT, acyl-CoA:cholesterol acyl-transferase

ALLN, N-acetyl-Leu-Leu norleucinal

BMP, bis(monooleoylglycero)phosphate

BSA, bovine serum albumin

CHO, Chinese hamster ovary

CMC, critical micellar concentration

CMV, cytomegalovirus

COP II, coat protein complex II

DMEM, Dulbecco's modified Eagle's medium

Endo H, endogylcosidase H

ER, endoplasmic reticulum

FCS, fetal calf serum

HMG-CoA, 3-hydroxy-3-methylglutaryl-coenzyme A

HSV, herpes simplex virus

LDL, low density lipoprotein

LPDS, lipoprotein-deficient serum

Ni-NTA, nickel-nitrilotriacetic acid

NP-40, nonidet P-40

NPC, Niemann-Pick Type C

NPC1, Niemann-Pick Type C1 disease protein

NPC1(NTD), N-terminal domain of NPC1 (amino acids 23-264)

NPC2, Niemann-Pick Type C2 disease protein

NTD, N-terminal domain

PBS, phosphate-buffered saline

PC, egg yolk L-α-phosphatidylcholine

PNGase F, Peptide: N-Glycosidase F

Scap, SREBP cleavage-activating protein

SREBP, sterol regulatory element-binding protein

Texas Red dye, Texas Red 1,2,-dihexadecanoyl-sn-glycero-3-phosphoethanolamine

TK, thymidine kinase

WT, wild-type

25-HC, 25-hydroxycholesterol

β-VLDL, β-migrating very low density lipoprotein

CHAPTER ONE

INTRODUCTION TO INTRACELLULAR CHOLESTEROL TRANSPORT

THE CHOLESTEROL TRANSPORT PATHWAY

Cholesterol is introduced to cells through either the diet or *de novo* synthesis. Endogenous cholesterol synthesis occurs in the ER, while cholesterol obtained from the diet is transported to cells as cholesteryl esters in low density lipoproteins (LDL) particles (Brown and Goldstein, 1986). This LDL enters cells through receptor mediated endocytosis mediated by the LDL-receptor, and is then sent to the endocytic compartment (Chang et al., 2006). Once in the endocytic compartment, acid lipase cleaves the cholesteryl ester to cholesterol and the free fatty acid. Subsequently, the free cholesterol then transverses the lysosome and is distributed among various membranes, including the ER.

Whether it is obtained from the diet or from *de novo* synthesis, cholesterol localizes to the ER, where it serves a regulatory role in cholesterol homeostasis. In the ER, these regulatory functions include activation of acetyl-coenzyme A acetyltransferase (ACAT), which is responsible for esterification of cholesterol for storage, and regulation of sterol regulatory element–binding proteins (SREBPs), membrane-bound transcription factors that regulate key enzymes required for cholesterol synthesis (Brown and Goldstein, 1997).

In cholesterol depleted cells, SREBPs are transported to the Golgi where they undergo two successive proteolytic cleavages, resulting in release of transcriptionally active forms into cytosol from which they migrate into the nucleus. This transcription factor then acts to increase transcription of genes encoding cholesterol biosynthetic enzymes (such as HMG-CoA reductase) and the LDL receptor. Additionally, ACAT activity is decreased, lowering the amount of free

cholesterol used for storage. When cholesterol in the ER membranes is abundant, ACAT is activated, thereby increasing the amount of cholesterol converted to cholesteryl esters for storage. In addition, high membrane cholesterol causes Scap to bind ER membrane proteins called Insigs; this interaction anchors SREBP in ER membranes, thereby preventing its proteolytic activation. Both processes are of high importance because they prevent the buildup of free insoluble cholesterol, which is toxic. This is summarized below.

FIGURE 1-1

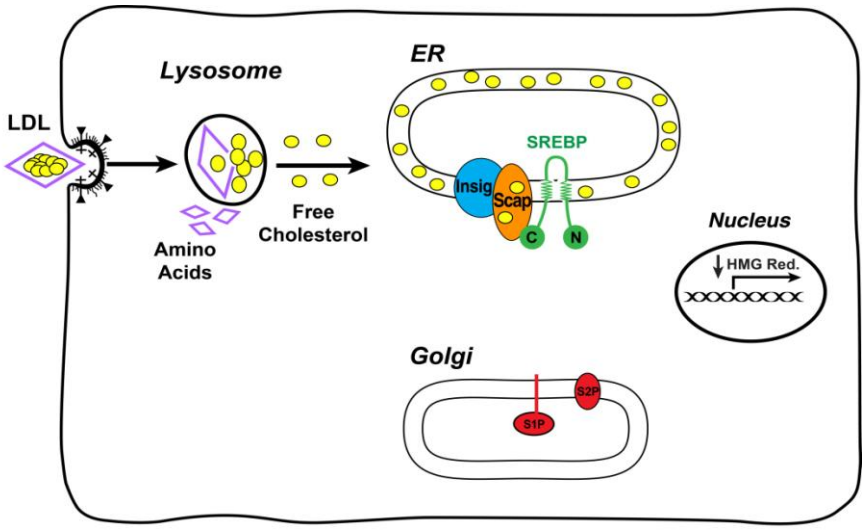

FIGURE 1-1. Movement and Effect of LDL-derived Cholesterol.

NIEMANN-PICK TYPE C PROTEINS

A clue to how LDL-derived cholesterol is transported to the ER from lysosomes comes from Niemann-Pick Type C (NPC) disease. NPC disease is a rare autosomal recessive lysosomal storage disease characterized by progressive central nervous system neurodegeneration, motor skill deficiencies, hepatosplenomegaly, and pulmonary complications (Vanier and Millat, 2003). NPC disease is fatal prior to adulthood owing to lipid buildup in lysosomes, including sphingolipids and unesterified cholesterol.

This NPC phenotype is indistinguishable whether the homozygous mutation occurs in either NPC2 or NPC1. This observation suggests that NPC2 and NPC1 function in the same pathway, namely export of cholesterol from lysosomes.

NPC1 AND NPC2

Human NPC1 is a protein of 1278 amino acids predicted to span the late endosomal membrane 13 times. Additionally, NPC1 is localized to late endosomes and contains a sterol-sensing domain (Loftus et al., 1997). NPC2 is a soluble protein of 132 amino acids that uses the mannose-6-phosphate marker for targeting to late endosomes (Chang et al., 2005). As NPC2 and NPC1 are exporters of cholesterol, both bind to cholesterol (Infante et al., 2008a; Xu et al., 2007). Furthermore, the cholesterol binding activity of NPC1 has been localized to the NH_2-terminal domain (NTD), not to the sterol-sensing domain. This domain can be expressed as a soluble protein of 240 amino acids (Infante et al., 2008b).

A detailed summary of the biochemical analysis and crystal structures of NPC2 and NPC1(NTD) provides a better understanding of their roles (Kwon et al., 2009; Xu et al., 2007). The structures of NPC2 and NPC1 (NTD) shows that NPC2 binds cholesterol with the iso-octyl chain facing the interior of the protein, whereas, NPC1(NTD) binds cholesterol with the 3ß-hydroxyl facing the interior of the protein. Another stark difference between NPC1 and NPC2 is the kinetics of their cholesterol binding. NPC2 binds and releases cholesterol rapidly (half-time < 2 min at 4^oC), while NPC1 (NTD) binds cholesterol very slowly (half-time > 2 hr at 4^oC) (Infante et al., 2008b). However, NPC2 can stimulate cholesterol binding to NPC1 (NTD) (>15-fold *in vitro*).

The stimulation of NPC1 (NTD) binding by NPC2 is believed to occur through a direct transfer of cholesterol. To help confirm this transfer hypothesis, an alanine scan mutagenesis was performed on NPC1 (NTD) (Kwon et al., 2009). Residues key for cholesterol binding were identified and shown to map the cholesterol binding pocket. Also, residues important for the NPC2 stimulation of NPC1(NTD) binding, but not NPC1(NTD) binding, were identified. These residues map to a discrete region near the opening of the cholesterol binding pocket. The most informative and well characterized of these NPC1 mutants is L175Q/L176Q (Kwon et al., 2009). These data lends support to the hypothesis that NPC2 directly transfers cholesterol to NPC1(NTD).

To further confirm the direct transfer hypothesis, we performed an alanine scan mutagenesis on NPC2. We identified residues key to cholesterol binding that map to the cholesterol binding pocket. Further, residues important for the NPC2 stimulation of NPC1(NTD) binding, but not NPC2 binding, were identified. These residues also mapped to a hydrophobic patch near the opening of the cholesterol binding pocket. Taken together, this evidence suggests that cholesterol is transported in the lysosome via a direct "handoff" of cholesterol from NPC2 to NPC1.

Scap

Maintaining cellular cholesterol homeostasis is of high importance, as a buildup of insoluble cholesterol is toxic. As described above, high cholesterol in ER membranes leads to formation of a Scap:Insig complex, which subsequently anchors SREBP in the ER membrane, thereby shutting down endogenous cholesterol synthesis. *In vitro* binding assays show that the membrane domain of Scap directly binds to cholesterol (Radhakrishnan et al., 2004), implicating

that Scap serves as the sensor that responds to intracellular cholesterol maintaining cholesterol homeostasis. The recombinant protein used for these assays consists of amino acid residues 1-767, containing two luminal loops separated by a sterol-sensing domain (Nohturfft et al., 1998).

As the cholesterol binding activity of Scap is of necessity for cell survival, we set out to further identify the region of Scap that recognizes cholesterol. The first loop region of Scap [Scap(Loop1)], but not the sterol-sensing domain, was shown to bind cholesterol with similar affinity and specificity to the membrane domain of Scap. Additionally, we performed an alanine scan mutagenesis of Scap(Loop1) using a cell-based assay and demonstrated that this loop region of Scap contains residues important for cholesterol responsiveness but not for cholesterol binding. This result suggests that Scap(Loop1) senses cellular cholesterol through direct interaction with the sterol, which results in a conformational change in Scap that anchors SREBPs in the membrane.

CHAPTER TWO

THE CHOLESTEROL BINDING AND TRANSFER ACTIVITY OF NPC2 IS CRUCIAL FOR CHOLESTEROL EXPORT FROM LYSOSOMES

SUMMARY

Water-soluble Niemann-Pick C2 (NPC2) and membrane-bound NPC1 are cholesterol-binding lysosomal proteins required for export of lipoprotein-derived cholesterol from lysosomes. The binding site in NPC1 is located in its N-terminal domain (NTD), which projects into the lysosomal lumen. Here, we perform alanine-scanning mutagenesis to identify residues in NPC2 that are essential for transfer of cholesterol to NPC1(NTD). Transfer requires three residues that form a patch on the surface of NPC2. We previously identified a patch of residues on the surface of NPC1(NTD) that are required for transfer. We present a model in which these two surface patches on NPC2 and NPC1(NTD) interact, thereby opening an entry pore on NPC1(NTD) and allowing cholesterol to transfer without passing through the water phase. We refer to this transfer as a hydrophobic handoff and hypothesize that this handoff is essential for cholesterol export from lysosomes.

INTRODUCTION

Low density lipoproteins (LDL) and related plasma lipoproteins deliver cholesterol to cells by receptor-mediated endocytosis. The lipoprotein is degraded in late endosomes and lysosomes where its cholesterol is released (Brown and Goldstein, 1986). Egress of cholesterol from late endosomes and lysosomes (hereafter referred to as lysosomes) requires two proteins: Niemann-Pick C2 (NPC2), a soluble protein of 132 amino acids (Naureckiene et al., 2000); and NPC1, an intrinsic membrane protein of 1278 amino acids and 13 postulated membrane-spanning helices that span the lysosomal membrane (Carstea et al., 1997; Pentchev, 1995). Recessive loss-of-function mutations in either NPC2 or NPC1 produce NPC disease, which causes death in childhood owing to cholesterol accumulation in lysosomes of liver, brain, and lung (Pentchev, 1995).

In keeping with their cholesterol export role, NPC2 and NPC1 both bind cholesterol (Infante et al., 2008a; Xu et al., 2007). Competitive binding studies (Infante et al., 2008b) and crystal structures (Kwon et al., 2009; Xu et al., 2007) indicate that the two proteins bind cholesterol in opposite orientations. NPC2 binds the iso-octyl side chain, leaving the 3β-hydroxyl exposed, whereas NPC1 binds the 3β-hydroxyl, leaving the side chain partially exposed. The cholesterol binding site on NPC1 is located in the NH_2-terminal domain (NTD), which projects into the lysosomal lumen. This domain, designated NPC1(NTD), can be expressed *in vitro* as a soluble protein of 240 amino acids that retains cholesterol binding activity (Infante et al., 2008b).

An important difference between NPC2 and NPC1(NTD) lies in the kinetics of sterol binding. When incubated at 4°C, NPC2 binds and releases cholesterol rapidly (half-time < 2 min) (Infante et al., 2008c). This rapid binding allows NPC2 to transfer cholesterol from one

liposome to another (Babalola et al., 2007). In contrast, at 4°C NPC1(NTD) binds cholesterol very slowly (half-time > 2 hr) (Infante et al., 2008c). Cholesterol binding to NPC1(NTD) is accelerated by >15-fold when the sterol is first bound to NPC2 and then transferred to NPC1(NTD). Unlike NPC2, NPC1(NTD) cannot rapidly transfer its bound cholesterol to liposomes (Infante et al., 2008c). However, NPC1(NTD) can accomplish this delivery when NPC2 is present (Infante et al., 2008c). These data led us to advance a model in which NPC2 can mediate bi-directional transfer of cholesterol to or from NPC1(NTD). In cells, we envision that NPC2 accepts cholesterol in the lysosomal lumen and transports it to membrane-bound NPC1, thus accounting for the requirement for both proteins for lysosomal cholesterol export (Infante et al., 2008c; Kwon et al., 2009).

The crystallographic structure of NPC1(NTD) with bound sterol gave a clue as to the possible requirement for NPC2. In NPC1(NTD), entrance into the cholesterol binding pocket is obstructed by α-helices that must move aside to permit entry or exit, thus explaining the slow binding of cholesterol when delivered in solution (Kwon et al., 2009). We envision that NPC2 binds to NPC1(NTD), displacing the helices and allowing direct transfer of cholesterol into the binding pocket of NPC1(NTD). This direct transfer avoids the necessity for insoluble cholesterol to transit the water phase. In the current study, we test this transfer hypothesis by producing mutant forms of NPC2 and NPC1(NTD) that can bind cholesterol but cannot engage in transfer from one protein to the other. These transfer mutants map to discrete regions on the surface of the two proteins that may be sites where the two proteins interact.

EXPERIMENTAL PROCEDURES

Materials – We obtained [1,2,6,7-^{3}H]cholesterol (60 or 100 Ci/mmol) from American Radiolabeled Chemicals; anti-FLAG M2-Agarose affinity beads, FLAG peptide, and anti-FLAG M2 antibody from Sigma; Nonidet P-40 from Roche Applied Sciences; Ni-NTA-agarose beads from Qiagen; egg yolk L-α-phosphatidylcholine (PC) and Texas Red dye from Avanti Polar Lipids; Cellgro ITS (insulin, transferrin, selenium) from Mediatech, Inc.; glycosidase Endo H and PNGase F from New England Biolabs; Superdex 200 10/300 GL columns from GE Healthcare Biosciences; and Bovine Serum Albumin Standard (2 mg/ml) from Thermo Scientific. Reagents and lipoproteins for assays of cholesterol esterification were as previously described (Goldstein et al., 1983; Infante et al., 2008a).

Buffers and Media – Buffer A contained 50 mM MES (pH 5.5 or 6.5) and 150 mM NaCl. Buffer B contained 50 mM Tris-chloride (pH 7.4) and 150 mM NaCl. Buffer C contained 10 mM HEPES (pH 7.6), 1.5 mM $MgCl_2$, 10 mM KCl, 5 mM sodium EDTA, 5 mM sodium EGTA, and 250 mM sucrose. Buffer D contained 10 mM Tris-chloride (pH 6.8), 100 mM NaCl, and 0.5% (w/v) SDS. Buffer E contained 62.5 mM Tris-chloride (pH 6.8), 15% SDS, 8 M urea, 10% (v/v) glycerol, and 100 mM DTT. Medium A contained a 1:1 mixture of Ham's F12 medium and DMEM, 100 units/ml penicillin, and 100 μg/ml streptomycin sulfate. Medium B contained DMEM, 100 units/ml penicillin, and 100 μg/ml streptomycin sulfate.

Plasmid Construction – Four previously described plasmids were used in these studies. All 4 are under the control of the CMV promoter. pCMV-NPC1-His8-FLAG encodes wild type (WT) human NPC1 followed sequentially by 8 histidines and a FLAG tag (Infante et al., 2008a). pCMV-NPC1(1-264)-LVPRGS-His8-FLAG encodes the N-terminal domain of WT human NPC1 (amino acids 1-264) followed sequentially by a thrombin cleavage site (LVPRGS), 8

histidines, and a FLAG tag (Infante et al., 2008c). pCMV-NPC2-His10 encodes WT human NPC2 (amino acids 1-151) followed by 10 histidines (Infante et al., 2008b). pCMV-NPC2-FLAG encodes WT human NPC2 (amino acids 1-151) followed by a FLAG tag (Infante et al., 2008c).

Mutations in the above plasmid constructs were generated by site-directed mutagenesis (Stratagene QuikChange kit). The coding regions of all plasmids were sequenced to confirm the integrity of each construct.

Purification of Epitope-Tagged NPC1(NTD) and NPC2 from Medium of Transfected CHO Cells – NPC proteins were purified from the media of stably or transiently transfected CHO-K1 cells where they are secreted into the media (Infante et al., 2008c). NPC proteins containing a histidine tag (with or without a FLAG tag) were purified by Ni-NTA-agarose and gel filtration chromatography; NPC proteins with only a FLAG tag were purified by anti-FLAG M2 agarose and gel filtration chromatography. Plasmids used in the stably transfected cells were WT versions of pCMV-NPC1(1-264)-LVPRGS-His8-FLAG and pCMV-NPC2-FLAG. Plasmids used for transient transfections were mutant versions of pCMV-NPC1(1-264)-LVPRGS-His8-FLAG, mutant versions of pCMV-NPC2-FLAG, and WT and mutant versions of pCMV-NPC2-His10. The concentration of purified protein was determined with the BCA assay (Smith et al., 1985).

[^{3}H]Cholesterol Binding Assay – This assay was previously described (Infante et al., 2008b). Incubation conditions are detailed in figure legends. After incubation for the indicated time at 4°C, each reaction was diluted 5-fold with ice-cold buffer B containing 0.004% (v/v) NP-40, loaded onto a 2-ml Bio-Spin column (Bio-Rad) packed with 0.3 ml of Ni-NTA-agarose beads that had been preequilibrated with buffer B containing 0.004% NP-40. The beads were washed

with either 5 ml buffer B with 1% NP-40 for NPC1(NTD) or 6 ml buffer B with 0.004% NP-40 for NPC2. Protein-bound [^{3}H]cholesterol was eluted with 1 ml buffer B containing 250 mM imidazole and 1 or 0.5% NP-40 for NPC1(NTD) and NPC2, respectively, and quantified by scintillation counting.

Preparation of Complexes of [^{3}H]Cholesterol:NPC1(NTD) and [^{3}H]Cholesterol:NPC2 – To prepare material for the [^{3}H]cholesterol dissociation assays, we incubated 500 nM [^{3}H]cholesterol (132 x 10^3 dpm/pmol) and 30 μg NPC2-His10 in a final volume of 300 μl of buffer A (pH 5.5). To prepare material for the [^{3}H]cholesterol transfer assays, we incubated 500 nM [^{3}H]cholesterol (132 x 10^3 or 222 x 10^3 dpm/pmol) in a final volume of 500 μl buffer A (pH 5.5) with one of the following proteins: 20 μg NPC2-His10, 30 μg NPC2-FLAG, or 100 μg NPC1(NTD)-LVPRGS-His8-FLAG. After incubation for 10 min at 37°C and then 30 min at 4°C, the solution was passed at 4°C through a 24-ml Superdex-200 column that had been preequilibrated with buffer A (pH 5.5). Protein-bound [^{3}H]cholesterol emerged between 15.5 and 18.5 ml for NPC2 and between 13.5 and 16.5 ml for NPC1(NTD). The respective pooled fractions were used for the [^{3}H]cholesterol dissociation and transfer assays described below.

[^{3}H]Cholesterol Dissociation Assay – [^{3}H]Cholesterol:NPC2-His10 was isolated at 4°C (3 ml), diluted 9-fold with ice-cold buffer A (pH 6.5) containing 0.004% NP-40 and 11.25 μM unlabeled cholesterol and then incubated at 4 or 37°C. At the indicated time, a 1-ml aliquot of the pooled 27-ml sample was transferred to a tube containing 600 μl of Ni-NTA-agarose beads. After incubation for 3 min at 4°C, the beads were centrifuged at 800 x *g* for 1 min at room temperature, after which the supernatant was assayed for radioactivity.

[^{3}H]Cholesterol Transfer Assays – Three types of transfer assays were performed. Incubation conditions for the assays are detailed in figure legends. Assay A involves the transfer

of [^{3}H]cholesterol from donor NPC2-FLAG to acceptor NPC1(NTD)-LVPRGS-His8-FLAG. After incubation for 10 min at 4°C, each 100 μl reaction mixture was diluted with 500 μl of ice-cold buffer B and loaded onto a 2-ml column packed with 0.3 ml Ni-NTA-agarose beads that had been preequilibrated with buffer B. Each column was washed with 3 ml buffer B, after which NPC1(NTD)-LVPRGS-His8-FLAG was eluted with 1 ml buffer B containing 250 mM imidazole. The amount of [^{3}H]cholesterol transferred to NPC1(NTD)-LVPRGS-His8-FLAG was quantified by scintillation counting of the eluate.

Assay B involves the transfer of [^{3}H]cholesterol from donor NPC2-His10 to acceptor NPC1(NTD)-LVPRGS-His8-FLAG. After incubation for 10 min at 4°C, each 200-μl reaction mixture was diluted with 500 μl of ice-cold buffer B and loaded onto a 2-ml column packed with 0.2 ml of anti-FLAG M2-agarose beads that had been preequilibrated with buffer B. Each column was washed with 3 ml buffer B, after which NPC1(NTD)-LVPRGS-His8-FLAG was eluted with 1 ml buffer B containing 0.1 mg/ml FLAG peptide. The amount of [^{3}H]cholesterol transferred to NPC1(NTD)-LVPRGS-His8-FLAG was quantified by scintillation counting of the eluate.

Assay C involves the transfer of [^{3}H]cholesterol from donor NPC1(NTD) to acceptor PC liposomes. PC liposomes labeled with Texas Red dye were prepared as described (Infante et al., 2008c). After incubation for 10 min at 4°C, each reaction was diluted with 750 μl ice-cold buffer B, loaded onto a 2-ml column packed with 0.3 ml Ni-NTA-agarose beads that had been preequilibrated with buffer B, and then washed with 1 ml buffer B. The amount of [^{3}H]cholesterol transferred to liposomes was quantified by scintillation counting of the flow-through plus 1 ml buffer B wash.

Alanine Scan Mutagenesis of NPC2 – We prepared 57 plasmids encoding mutant forms of NPC2 in which 1, 2, or 3 sequential amino acids were changed to alanine by site-directed mutagenesis (Stratagene QuikChange kit). (Amino acid residues are numbered starting at the initiator methionine, which is designated no. 1.) To evaluate the NPC2 proteins encoded by these plasmids, the plasmids were transfected into CHO-K1 cells, after which assays for [^{3}H]cholesterol binding and transfer were performed with the secreted proteins. CHO-K1 cells were grown in monolayer at 37°C in 8-9% CO_2. On day 0, cells were plated at a density of 6 x 10^6 cells per 100-mm dish in medium A containing 5% (v/v) FCS. On day 2, dishes were transfected with 5 μg pcDNA3.1 or pCMV-NPC2-His10 (WT or mutant versions) as described (Rawson et al., 1999). On day 3, each dish was washed once with 10 ml Dulbecco's PBS and then switched to 7 ml medium A containing 1% (v/v) ITS. On day 6, the media from 5 dishes (35 ml) was collected and concentrated to 0.5 ml using a 10-kDa Amicon Ultra-15 Centrifugal Filter Unit (Millipore). The amount of secreted NPC2 in the concentrated media was estimated by densitometric scanning of immunoblots with anti-NPC2 antibody. Aliquots of the concentrated media containing either WT or mutant version of NPC2-His10 were used for the [^{3}H]cholesterol binding and transfer assays.

Cholesterol Esterification Assay in Intact Cells – Cholesterol esterification assays were performed with human fibroblasts as described (Goldstein et al., 1983). On day 0, control and NPC2-deficient fibroblasts (GM 18455; compound heterozygote with mutant alleles E20X and C47F; obtained from Coriell Institute for Medical Research) were set up in medium B containing 10% FCS at 25 x 10^3 and 100 x 10^3 cells/60-mm dish, respectively, and grown in monolayer at 37°C in 5% CO_2. On day 3, cells were refed with the same medium. On day 5, cells were washed once with PBS and switched to medium B containing 10% human lipoprotein-deficient

serum and 1% ITS. On day 7, cells were used for experiments. After incubation for 5 hr at 37°C with various additions as described in figure legends, each cell monolayer was pulse-labeled for 1 hr with 0.2 mM sodium [^{14}C]oleate. The rate of incorporation of [^{14}C]oleate into cholesteryl [^{14}C]oleate and [^{14}C]triglycerides by intact cell monolayers was measured as described (Goldstein et al., 1983; Kwon et al., 2009).

Cholesterol esterification assays were also performed in mutant CHO 4-4-19 cells defective in NPC1 function (Dahl et al., 1992). Cells were set up for experiments at 400 x 10^3 cells/60-mm dish in medium A with 5% FCS, transfected with 2-2.5 μg of the indicated plasmid on day 1 as described (Infante et al., 2008b), and incubated with various additions as described in figure legends, after which the incorporation of [^{14}C]oleate into cellular cholesteryl [^{14}C]oleate and [^{14}C]triglycerides was determined.

Glycosidase Treatment – 48 hr after transfection, NPC1-deficient CHO 4-4-19 cells were harvested, washed with PBS, and lysed in 200 μl buffer C containing 5 μg/ml pepstatin, 10 μg/ml leupeptin, and 1.9 μg/ml aprotinin by passing through a 22 gauge needle 30 times. The lysate was centrifuged at 2200 rpm for 5 min at 4°C. The supernatant was then centrifuged at 100,000 x *g* for 30 min at 4°C. The pellet was then resuspended in 100 μl buffer D and shaken for 30 min at room temperature. Reactions, in a final volume of 100 μl buffer D, contained 40 μl of solubilized membranes, 0.16 mM dithiothreitol in the absence or presence of 5000 U Endo H or 2500 U PNGase F. After incubation at 37°C for 3 hr, an equal volume of buffer E was added to each reaction, and the incubation at 37°C was continued for 30 min. Samples were then subjected to 8% SDS-PAGE and immunoblot with monoclonal anti-FLAG antibody.

Immunoblot Analysis – Samples for immunoblotting were subjected to 8% or 13% SDS-PAGE, after which the proteins were transferred to nitrocellulose filters. The immunoblots were

performed at room temperature using the following primary antibodies: 1 μg/ml mouse monoclonal anti-FLAG M2 (Sigma) and 1:3000 dilution of a rabbit antiserum directed against human NPC2. The latter antibody was raised by injecting rabbits with a His10-tagged recombinant version of the antigen. Bound antibodies were visualized by chemiluminescence (SuperSignal West Pico Chemiluminescent Substrate, Thermo Scientific) using a 1:5000 dilution of anti-mouse IgG (Jackson ImmunoResearch Laboratories, Inc.) or anti-rabbit IgG (GE Healthcare) conjugated to horseradish peroxidase. The films were exposed to Phenix Research Products Blue X-ray Film (F-BX810) at room temperature.

RESULTS

Alanine Scan Mutagenesis to Identify Residues of NPC2 Required for Cholesterol Binding and Transfer – To establish an assay to screen for residues in NPC2 that are essential for cholesterol binding or transfer to NPC1(NTD), we transfected CHO-K1 cells with plasmids encoding histidine-tagged wild-type or mutant NPC2. Like other lysosomal proteins (Kornfeld, 1987), a portion of NPC2 was secreted into the culture medium. To measure binding ability, aliquots of media were incubated with [^{3}H]cholesterol, and the NPC2-bound sterol was isolated by nickel chromatography. When cells expressed wild-type NPC2, the His-tagged NPC2 in the medium bound [^{3}H]cholesterol, whereas medium from mock-transfected cells showed no binding (Figure 2-1A). To measure cholesterol transfer, we used a previously described liposome transfer assay (Infante et al., 2008c). First, purified NPC1(NTD) was incubated with [^{3}H]cholesterol, and the bound sterol was separated from free [^{3}H]cholesterol by gel filtration chromatography as described in Experimental Procedures. The isolated [^{3}H]cholesterol:NPC1(NTD) complex was then incubated with phosphatidylcholine (PC)

liposomes, and the amount of [^{3}H]cholesterol transferred to liposomes was measured. In the presence of culture medium from mock-transfected cells, NPC1(NTD) failed to transfer its bound [^{3}H]cholesterol to liposomes (Figure 2-1B). Transfer was markedly stimulated in the presence of culture medium containing WT NPC2.

We next prepared 57 plasmids encoding mutant forms of NPC2 in which 1, 2, or 3 sequential amino acids were changed to alanine. (Amino acid residues are numbered starting at the initiator methionine, which is designated no. 1; the first residue after signal peptide cleavage is no. 20.) Our mutant panel included all residues in NPC2 that are exposed to the surface (Xu et al., 2007). We did not mutate any of the 6 cysteines, as to avoid disrupting disulfide bonds, or the single residue that was already alanine. We also did not mutate P120. When P120 is changed to serine, as in certain patients with NPC2 disease (Verot et al., 2007), binding of [^{3}H]cholesterol is abolished (Infante et al., 2008c). The mutant plasmids were introduced into CHO-K1 cells by transfection. We assayed aliquots of culture media that contained equivalent amounts of NPC2 as determined by immunoblotting. Thirteen of the 57 NPC2 mutant proteins showed binding that was less than 15% of the WT value determined in the same experiment (Figure 2-1C, blue). As shown in blue (with the exception of P100, which is remote), these mutations replaced residues that surround the sterol-binding pocket as delineated in the crystal structure of Xu, et al. (Xu et al., 2007) (Figure 2-1E). Moreover, the results of our mutant screen are consistent with the three binding mutants identified by Ko, et al. (2003), who used a different screening assay based on complementation by endocytosis of heterologously expressed mutant NPC2 proteins (Ko et al., 2003). Their binding mutants (F66, V96, and Y100) correspond in our numbering scheme to residues F85, V115, and Y119. In our screen, F85A and Y119A gave binding values of 3% and 8% of WT. Amino acid V115 was not included in our alanine scan,

but the two adjacent residues, P114 and K116, when mutated to alanine, gave binding values of 15% and 5% as compared to WT (Figure 2-1C).

We used the liposome transfer assay to analyze transfer activity in culture media from all of the alanine scan mutants whose [^{3}H]cholesterol binding activity exceeded 50% of WT (Figure 2-1D). Three of these mutants exhibited transfer activity that was less than 40% of WT (Figure 2-1D, red). All three of these closely spaced residues map to a surface patch on NPC2 that is adjacent to the opening of the cholesterol binding pocket (Figure 2-1E, red). When the alanine scan was repeated in its entirety in an independent experiment, the same three mutants were identified, and none of the other tested mutants showed defective transfer activity.

Biochemical Characterization of NPC2 Cholesterol Transfer Mutant – To further explore the transfer defect detected in the mutant screen, we studied additional amino acid substitutions at the valine-81 position. We used nickel affinity and gel filtration chromatography to purify His-tagged WT and mutant NPC2 proteins from culture media. Increasing amounts of purified WT NPC2 stimulated transfer of [^{3}H]cholesterol from NPC1(NTD) to liposomes, whereas the V81A mutant was less effective (Figure 2-2A). When valine-81 was changed to aspartic acid (V81D), the transfer defect was even greater (Figure 2-2A). Figure 5-2B shows the results of a 2-hr equilibrium binding assay at 4°C, indicating that the V81A and V81D mutants both bound cholesterol with affinities indistinguishable from WT. The calculated K_d values were 81, 80, and 72 nM for WT, V81A, and V81D, respectively. The V81D mutant and the WT protein showed identical rates of association with [^{3}H]cholesterol at 4°C (Figure 2-2C). To measure dissociation rates, we first isolated a [^{3}H]cholesterol:NPC2 complex by gel filtration, then diluted the complex, and then measured the rate of dissociation of bound [^{3}H]cholesterol. Both proteins exhibited identical dissociation rates at 4°C, and both were markedly accelerated at 37°C (Figure

2-2D). We used the isolated [^{3}H]cholesterol:NPC2 complexes as donors to measure the direct transfer of [^{3}H]cholesterol to NPC1(NTD) (Figure 2-2E). The V81A mutant was partially defective in this transfer and the V81D mutant was severely defective.

NPC2 Cholesterol Binding and Transfer Mutants Fail to Restore Function to NPC2-Deficient Cells – To confirm that the transfer mutants are defective in living cells, we measured the ability of WT and mutant NPC2 proteins to restore egress of LDL-derived cholesterol in fibroblasts from a patient with two defective NPC2 alleles. We incubated the cells with [^{14}C]oleate and measured the rate of its incorporation into cholesteryl [^{14}C]oleate, a reaction that requires movement of LDL-derived cholesterol from lysosomes to ER (Goldstein et al., 1983). In WT cells, LDL caused a marked increase in cholesteryl [^{14}C]oleate formation (Figure 2-3A), whereas the mutant NPC2 cells showed no response. Both cells responded to 25-hydroxycholesterol, which enhances cholesteryl [^{14}C]oleate synthesis in a fashion that does not require the lysosome. To correct the NPC2 phenotype in the mutant cells, we took advantage of the fact that NPC2 is a lysosomal protein that contains mannose-6-phosphate residues that mediate its cellular uptake and delivery to lysosomes (Chikh et al., 2004; Naureckiene et al., 2000). In the presence of LDL, addition of purified WT NPC2 protein to the culture medium led to a marked increase in cholesteryl [^{14}C]oleate synthesis in the mutant NPC2 cells (Figure 2-3B). There was little stimulation when we added the previously described cholesterol-binding mutant of NPC2 (P120S) (Infante et al., 2008c). We also found little stimulation with the cholesterol transfer mutant (V81D). None of these proteins influenced cholesteryl [^{14}C]oleate synthesis in control fibroblasts (Figure 2-3C). We repeated these experiments with NPC2 proteins that contained a FLAG epitope tag and observed identical results (data not shown). Immunoblotting

of cell extracts with anti-NPC2 confirmed the uptake of all three proteins in control and mutant fibroblasts (data not shown).

Biochemical Characterization of NPC1(NTD) Cholesterol Transfer Mutant – Previously, we described a mutation in NPC1(NTD) that did not alter cholesterol binding but partially reduced the ability of the NPC1(NTD) to transfer cholesterol to or from NPC2 (Kwon et al., 2009). This mutation converted two adjacent leucines to alanine (L175A/L176A). To increase this transfer defect, we changed the two leucines to glutamines (L175Q/L176Q). When incubated with [^{3}H]cholesterol in solution for 24 hr at 4°C, this mutant protein bound [^{3}H]cholesterol indistinguishably from WT (Figure 2-4A). However, when incubated with NPC2-bound [^{3}H]cholesterol for 10 min, WT NPC1(NTD) accepted the [^{3}H]cholesterol, whereas the L175Q/L176Q mutant was nearly devoid of acceptor activity (Figure 2-4B). Thus, the L175Q/L176Q mutant of NPC1(NTD) is analogous to the V81D mutant of NPC2. Both mutant proteins can bind cholesterol, but cannot transfer it to the other protein.

NPC1 Cholesterol Transfer Mutant Fails to Restore Function to NPC1-Deficient Cells – To confirm that the L175Q/L176Q mutation disrupted the function of NPC1 in living cells, we introduced this mutation into a plasmid encoding full-length NPC1. Plasmids encoding WT or L175Q/L176Q mutant NPC1 were transfected into CHO 4-4-19 cells, which are deficient in NPC1 (Dahl et al., 1992). To test for NPC1 function, we measured synthesis of cholesteryl [^{14}C]oleate after administration of β-VLDL, a cholesterol-rich lipoprotein that binds to hamster LDL receptors more avidly than does human LDL. In mock-transfected CHO 4-4-19 cells, β-VLDL did not stimulate cholesteryl ester synthesis (Figure 2-5A). Expression of WT NPC1 permitted a marked stimulation, whereas the L175Q/L176Q mutant was much less effective. The transfected cells expressed similar amounts of WT and L175Q/L176Q NPC1 as determined

by immunoblotting (Figure 2-5A, inset). In both proteins, the *N*-linked carbohydrate chains were partially resistant to treatment with Endo H, indicating that the proteins had folded properly and reached the Golgi apparatus. Treatment with PNGase F lowered the apparent molecular mass of both proteins as a result of removal of all *N*-linked carbohydrates (Figure 2-5B).

Free Cholesterol Does not Effectively Compete for the Transfer of [^{3}H]Cholesterol from NPC2 to NPC1(NTD) – To confirm that the transfer of [^{3}H]cholesterol from NPC2 to NPC1(NTD) is direct, we utilized a kinetic competition assay. We used the isolated [^{3}H]cholesterol:NPC2 complexes as donors to measure the direct transfer of [^{3}H]cholesterol to NPC1(NTD) in the presence of increasing amounts of free unlabeled cholesterol. When assayed at 3 minutes, the free cholesterol in the assay did not compete with the direct transfer of [^{3}H]cholesterol to NPC1(NTD) (Figure 2-6A). To determine if the free cholesterol was in solution and able to bind the NPC proteins in the assay, we carried out a time course on the transfer of [^{3}H]cholesterol from NPC2 to NPC1(NTD) in the presence of a 200-fold excess of unlabeled cholesterol. With increasing time, the free cholesterol was able to effectively bind NPC1(NTD) (Figure 2-6B).

FIGURE 2-1. Alanine Scan Mutagenesis of NPC2: [^{3}H]Cholesterol Binding and Transfer Activities.

(A and C) [^{3}H]Cholesterol binding to NPC2 in culture medium from transfected cells. Each reaction, in final volume of 160 μl, contained 110 μl buffer B, 50 μl concentrated medium as described in Experimental Procedures, 1.9 μg BSA, 0.004% NP-40, and [^{3}H]cholesterol (A, indicated concentration at 222 x 10^3 dpm/pmol; C, 200 nM at 132 x 10^3 dpm/pmol). After 2 hr at 4°C, the amount of bound [^{3}H]cholesterol was measured as described in Experimental Procedures except reactions were not diluted before loading onto Ni-NTA columns. (A) Each value represents total binding after subtraction of blank value (<0.03 pmol/tube). (C) Each bar is the average of duplicate assays, and represents binding relative to WT NPC2 studied in same experiment. All binding data were adjusted for variations (typically <2-fold) in the amount of secreted NPC2 protein as determined by densitometric scanning of immunoblots of the assayed protein in the eluate. The data in the graph were obtained in 5 separate experiments. The "100% of control" values (WT NPC2) averaged 1.5 pmol/tube (average value for mock-transfected cells in same 5 experiments was <0.1 pmol/tube). The entire alanine scan was repeated in an independent experiment with similar results. Blue bars denote residues that when mutated to alanine decrease binding by >85%. (B and D) [^{3}H]Cholesterol transfer from NPC1(NTD) to liposomes in presence of NPC2 contained in culture medium from transfected cells. Each reaction, in a final volume of 200 μl, contained 130 μl buffer A (pH 5.5), ~40 pmol of WT NPC1(NTD)-LVPRGS-His8-FLAG complexed to [^{3}H]cholesterol (132 x 10^3 dpm/pmol), 20 μg PC liposomes, and concentrated medium (B, 0-10 μl; D, 30 μl). After 10 min at 4°C, [^{3}H]cholesterol transferred to liposomes was measured as described in Experimental Procedures

(assay *C*). (B*)* Each value represents percentage of [^{3}H]cholesterol transferred after subtraction of percentage in absence of medium (11% transfer). The 100% value for transfer was 0.14 pmol/tube. (D) Each bar is the average of duplicate assays, and denotes percentage of [^{3}H]cholesterol transferred in presence of NPC2 after subtraction of percentage in absence of NPC2. The data in the graph were obtained in 5 separate experiments. The "100% of control" values (WT NPC2) averaged 38% transfer of total input (average value for mock-transfected cells in same 5 experiments was 1.8%). The entire alanine scan was repeated in an independent experiment with similar results. Red bars denote residues that when mutated to alanine decrease NPC2-mediated [^{3}H]cholesterol transfer by >60%. (E) Ribbon diagram of bovine NPC2 (Xu et al., 2007), showing positions of residues crucial for cholesterol binding (blue) and transfer (red). Residue P100 is only one of 14 residues important for binding [^{3}H]cholesterol that does not map to sterol-binding pocket. Residue 81 (Ile bovine sequence; Val in human) was identified in above alanine scan as essential for [^{3}H]cholesterol transfer, but not binding. Residue P120 was previously identified as essential for both binding and transfer (Infante et al., 2008c). Bound cholesterol sulfate is shown in green.

FIGURE 2-1

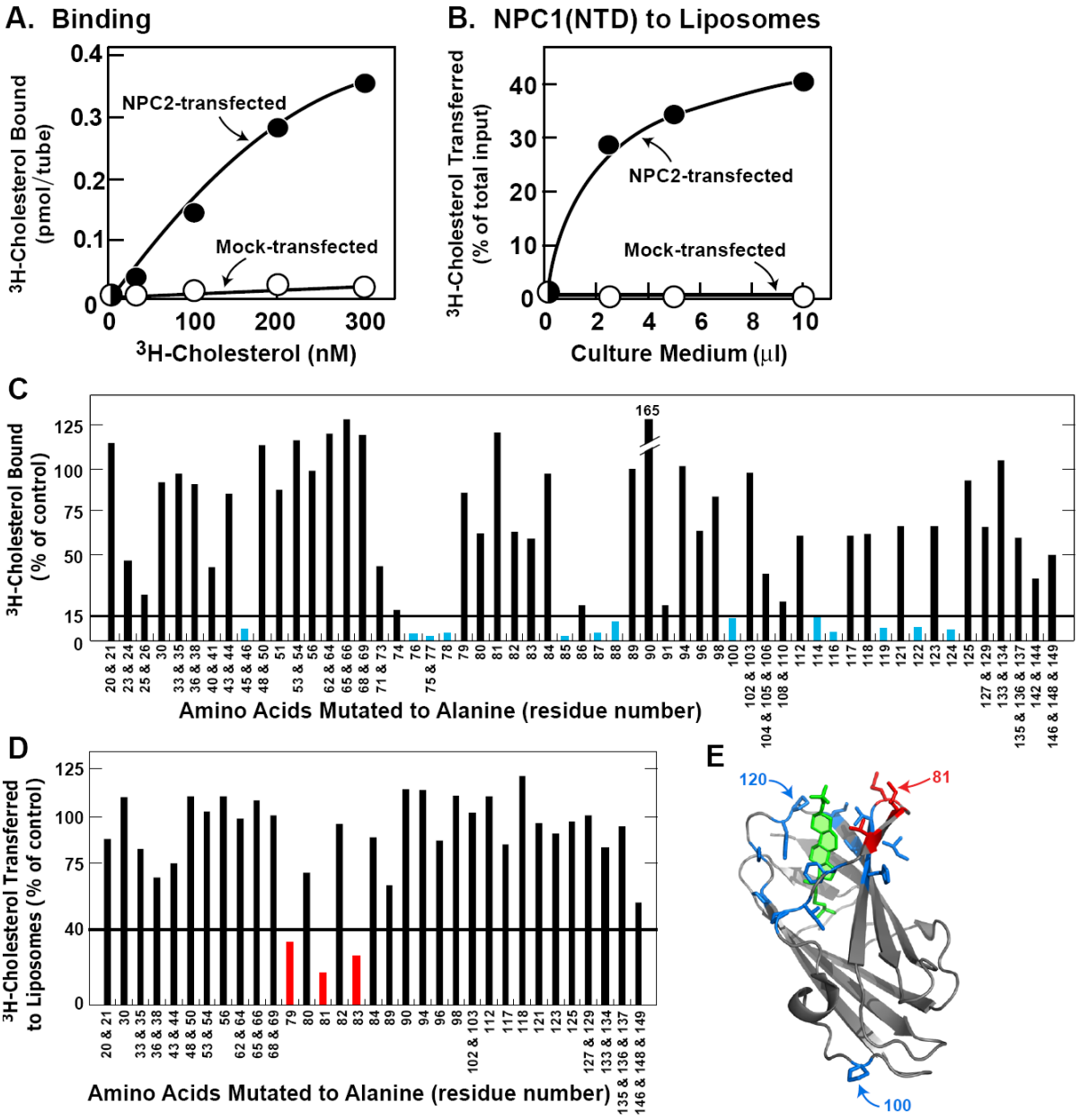
A. Binding
^{3}H-Cholesterol Bound (pmol/tube)
NPC2-transfected
Mock-transfected
^{3}H-Cholesterol (nM)
B. NPC1(NTD) to Liposomes
^{3}H-Cholesterol Transferred (% of total input)
NPC2-transfected
Mock-transfected
Culture Medium (μl)
C
^{3}H-Cholesterol Bound (% of control)
165
Amino Acids Mutated to Alanine (residue number)
D
^{3}H-Cholesterol Transferred to Liposomes (% of control)
Amino Acids Mutated to Alanine (residue number)
E
120
81
100

FIGURE 2-2. Biochemical Analysis of NPC2 Transfer-defective Mutants.

(A) [^{3}H]Cholesterol transfer from NPC1(NTD) to liposomes as a function of NPC2. Each reaction, in a final volume of 200 μl buffer A (pH 5.5), contained ~50 pmol of WT NPC1(NTD)-LVPRGS-His8-FLAG complexed to [^{3}H]cholesterol (222 x 10^3 dpm/pmol), 20 μg PC liposomes, and the indicated concentration of WT or mutant NPC2-His10. After 10 min at 4°C, [^{3}H]cholesterol transferred to liposomes was measured as described in Experimental Procedures (assay C). Each value represents percentage of [^{3}H]cholesterol transferred. A blank value in the absence of NPC2 (7% transfer) was subtracted. The 100% value for transfer was 1.9 pmol/tube. (B) [^{3}H]Cholesterol binding. Each reaction, in a final volume of 80 μl buffer A (pH 5.5) with 0.004% NP-40, contained 8 pmol of purified WT or mutant NPC2-His10, 1 μg BSA, and the indicated concentration of [^{3}H]cholesterol (222x10^3 dpm/pmol). After 2 hr at 4°C, bound [^{3}H]cholesterol was measured. Each value represents total binding after subtraction of blank value (<0.1 pmol/tube). (C) Time course of association of [^{3}H]cholesterol to NPC2. Each reaction, in a final volume of 80 μl of buffer A (pH 5.5) with 0.004% NP-40, contained 8 pmol of WT or mutant NPC2-His10 and 200 nM [^{3}H]cholesterol (132 x 10^3 dpm/pmol). After incubation for indicated time at 4°C, bound [^{3}H]cholesterol was determined. Each value represents total binding after subtraction of a blank value (<0.03 pmol/tube). (D) Dissociation of previously bound [^{3}H]cholesterol from NPC2 at different temperatures. Dissociation of [^{3}H]cholesterol from [^{3}H]cholesterol:NPC2-His10 (WT or mutant) was measured as described in Experimental Procedures. Each value represents the percentage of [^{3}H]cholesterol remaining bound to WT or mutant NPC2 relative to zero-time value. The ‘‘100% initial binding’’ values at zero time for NPC2 was 0.48 (WT) and 0.26 (mutant) pmol/tube. (E) [^{3}H]Cholesterol transfer from NPC2 to NPC1(NTD). Each reaction, in a final volume of 200 μl buffer A (pH 5.5),

contained ~40 pmol of WT or mutant NPC2-His10 complexed to [^{3}H]cholesterol (222 x 10^3 dpm/pmol) and the indicated concentration of WT NPC1(NTD)-LVPRGS-His8-FLAG. After 10 min at 4°C, [^{3}H]cholesterol transferred was measured as described in Experimental Procedures (assay *B*). Each value represents percentage of [^{3}H]cholesterol transferred to NPC1(NTD). Blank values in the absence of NPC1(NTD) (0.1-0.5% transfer) were subtracted. The 100% values for transfer from WT, V81A, and V81D NPC2 were 0.24, 0.78, and 0.29 pmol/tube, respectively. (A-E) Each value is the average of duplicate assays.

FIGURE 2-2

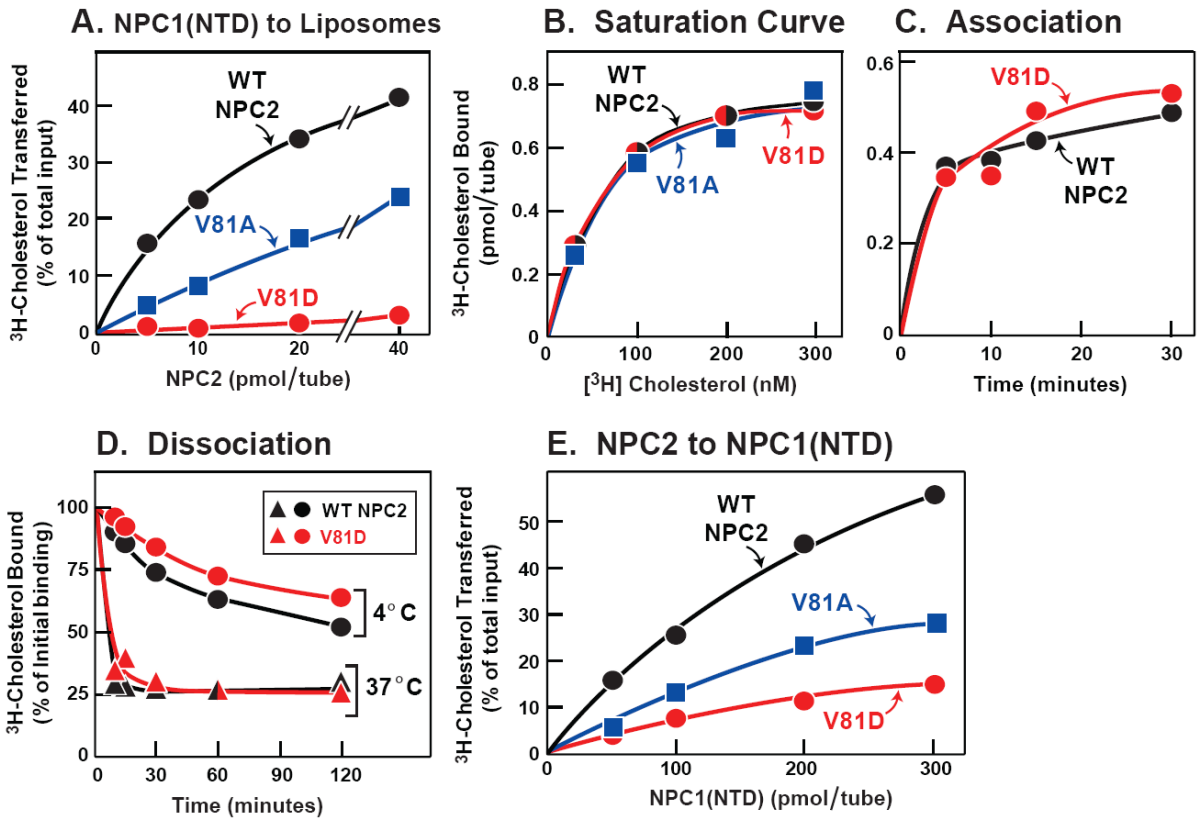

FIGURE 2-3. Ability of WT NPC2, but not Mutant NPC2, to Rescue LDL-stimulated Cholesteryl Ester Formation in NPC2-deficient Human Fibroblasts.

(A) Control and NPC2-deficient cells were set up for experiments as described in Experimental Procedures. On day 7, cells were switched to medium B containing 5% lipoprotein-deficient serum, 50 μM compactin, and 50 μM sodium mevalonate in the absence or presence of 10 μg/ml 25-hydroxycholesterol (25-HC) or 60 μg protein/ml LDL as indicated. (B and C) On day 7, cells were switched to above medium supplemented with 60 μg protein/ml LDL and indicated concentration of purified WT or mutant NPC2-His10. (A-C) After 5 hr at 37°C, each cell monolayer was pulse-labeled for 1 h with 0.2 mM sodium [^{14}C]oleate (3480 dpm/nmol), and cellular content of cholesteryl [^{14}C]oleate and [^{14}C]triglycerides were determined. Each value is the average of duplicate incubations. Content of [^{14}C]triglycerides in NPC2-deficient fibroblasts treated with 60 μg/ml LDL and 3 μg/ml of WT, V81D, or P120S NPC2-His10 proteins was 3.1, 3.0, and 4.0 nmol/hr per mg protein, respectively.

FIGURE 2-3

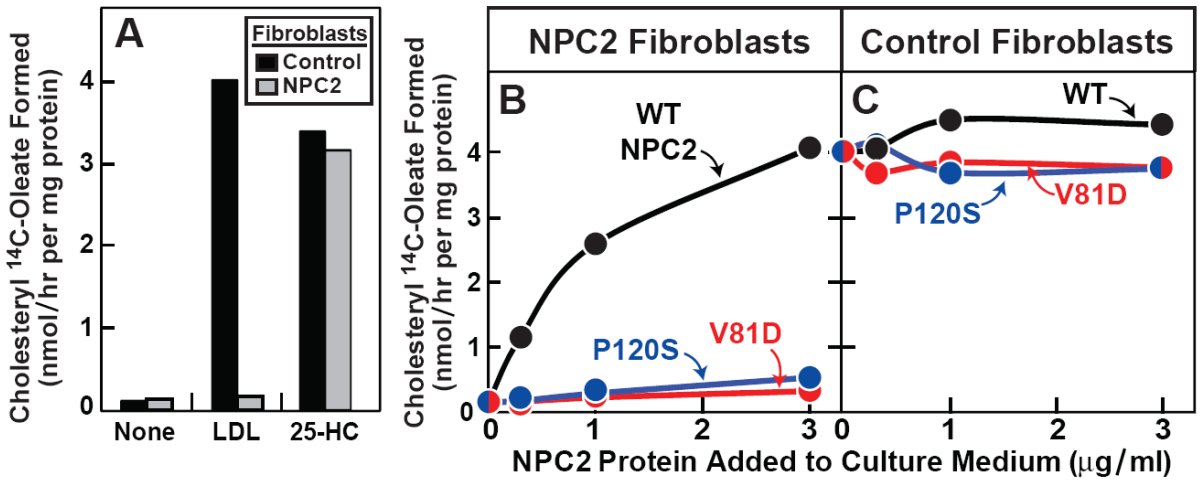

FIGURE 2-4. Biochemical Analysis of NPC1(NTD) Transfer-defective Mutant.

(A) [^{3}H]Cholesterol binding. Each reaction, in a final volume of 80 µl buffer A (pH 5.5) with 0.004% NP-40, contained 4 pmol purified WT or mutant NPC1(NTD)-LVPRGS-His8-FLAG, 1 µg BSA, and indicated concentration of [^{3}H]cholesterol (132 x 10^3 dpm/pmol). After 24 hr at 4°C, bound [^{3}H]cholesterol was measured. Each value represents total binding after subtraction of a blank value (<0.06 pmol/tube). (B) [^{3}H]Cholesterol transfer from NPC2 to NPC1(NTD). Each reaction, in a final volume of 100 µl buffer A (pH 5.5), contained ~24 pmol of NPC2-FLAG complexed to [^{3}H]cholesterol (132 x 10^3 dpm/pmol) and the indicated concentration of WT or mutant NPC1(NTD)-LVPRGS-His8-FLAG. After 10 min at 4°C, [^{3}H]cholesterol transferred was measured as described in Experimental Procedures (assay A). Each value represents percentage of [^{3}H]cholesterol transferred to NPC1(NTD). A blank value in the absence of NPC1(NTD) (0.3% transfer) was not subtracted. The 100% value for transfer from NPC2 was 0.85 pmol/tube. (A and B) Each value is the average of duplicate assays.

FIGURE 2-4

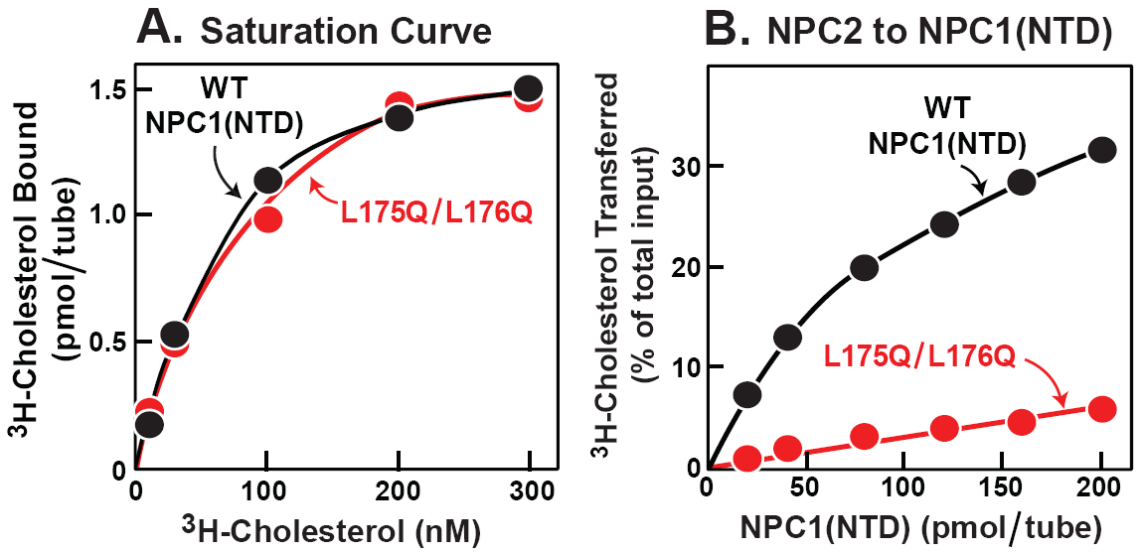

FIGURE 2-5. Failure of Mutant L175Q/L176Q Version of Full-length NPC1 to Rescue Cholesteryl Ester Formation in NPC1-defective Hamster Cells.

(A) Cholesterol esterification in response to β-VLDL. NPC1-deficient CHO 4-4-19 cells were transfected on day 1 with 2 μg pcDNA3.1 (mock), WT pCMV-NPC1-His8-FLAG, or its mutant version (L175Q/L176Q) as described in Experimental Procedures. Five hr after transfection, the medium was switched to medium A containing 5% newborn calf lipoprotein-deficient serum. On day 2, the medium was switched to same medium containing 5 μM compactin and 50 μM sodium mevalonate. After 16 hr, fresh medium containing 50 μM compactin, 50 μM sodium mevalonate, and the indicated concentration of β-VLDL was added. After 5 hr at 37°C, each monolayer was pulse-labeled for 1 hr with 0.2 mM sodium [^{14}C]oleate (7433 dpm/nmol). The cells were then harvested for measurement of their content of cholesteryl [^{14}C]oleate and [^{14}C]triglycerides as described in Experimental Procedures. Each value is the average of duplicate incubations. The content of [^{14}C]triglycerides for mock, WT, and mutant NPC1 transfected cells incubated with 10 μg/ml β-VLDL was 201, 222, and 129 nmol/hr per mg protein, respectively. Inset shows an immunoblot of whole cell extracts from the various transfected cells probed with anti-FLAG antibody as described in Experimental Procedures. (B) Deglycosidase treatment. NPC1-deficient CHO cells were transfected with the indicated plasmid as in (A). Five hr after transfection, the medium was switched to medium A with 5% FCS. Two days later, cells were harvested, and their solubilized membranes were treated with glycosidase Endo H or PNGase F and then subjected to immunoblot analysis with anti-FLAG antibody as described in Experimental Procedures. (A and B) Filters were exposed to film for ~10 sec at room temperature.

FIGURE 2-5

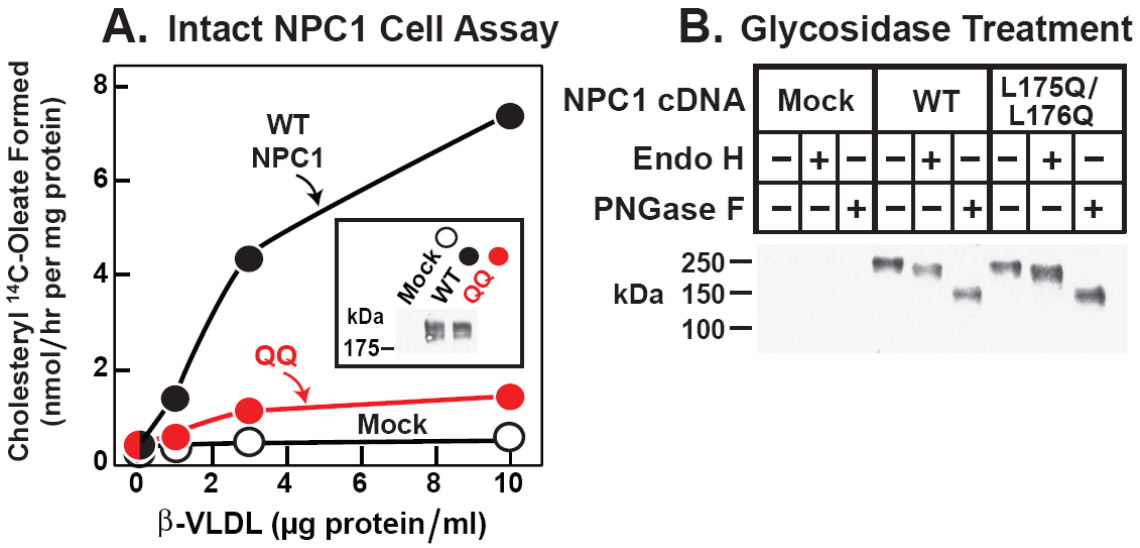

(Data for 2-5 A from Lina Abi-Mosleh)

FIGURE 2-6. Non-inhibition of Cholesterol Transfer from NPC2 to NPC1(NTD) by Excess Unlabeled Cholesterol.

Each reaction, in a final volume of 120 ul buffer A (pH 5.5) with 0.0004% NP-40, contained 120 pmol of WT NPC1(NTD)-LVPRGS-His_8-FLAG and ~4.5 nM [^{3}H]cholesterol (222x10^3 dpm/pmol) complexed to ~40 pmol NPC2-FLAG. (A) Each tube contained the indicated amount of unlabeled sterol. After incubation for 3 min at 4^{o}C, the amount of bound [^{3}H]cholesterol was determined as described. (B) Each tube contained either no unlabeled sterol or 100 pmol of unlabeled sterol. After incubation for the indicated time at 4^{o}C, the amount of bound [^{3}H]cholesterol was determined as described. Each value represents percentage of [^{3}H]cholesterol transferred from NPC2 to NPC1(NTD), and is the average of duplicate assays. Blank values were not subtracted.

FIGURE 2-6

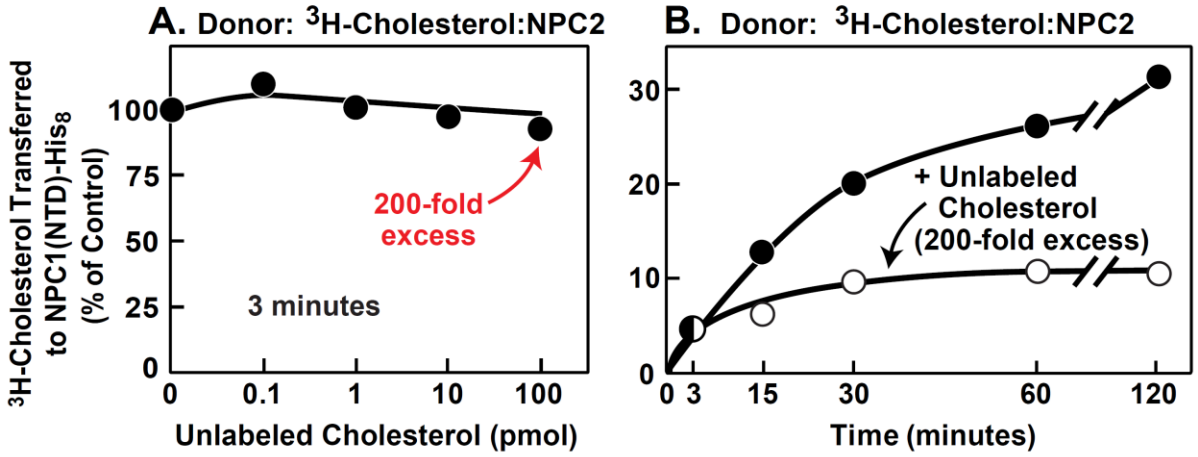

FIGURE 2-7. Conceptual Model Illustrating One Possible Mechanism of Interaction Between NPC2 and NPC1(NTD).

This model is based on the published structures of sterol-bound NPC2 (Xu et al., 2007) and sterol-bound NPC1(NTD) in the putative open conformation (Kwon et al., 2009). A stable complex between NPC2 and NPC1(NTD) has not been demonstrated experimentally, and the interaction models in A and B are hypothetical. (A) Surface representation showing residues in NPC2 (purple) and NPC1(NTD) (green) that are crucial for transfer of cholesterol (red) between NPC2 and NPC1(NTD). The cholesterol molecule is shown after its transfer to NPC1(NTD). The two proteins are positioned so that the openings in their respective sterol-binding pockets are juxtaposed and the planes of the cholesterol-binding pockets in NPC2 and NPC1(NTD) are aligned. (B) Cutaway view of the NPC2:NPC1(NTD) complex shown in A, revealing alignment of the cholesterol-binding pockets and juxtaposition of the surface patches on both proteins postulated to be crucial for protein-protein interaction.

FIGURE 2-7

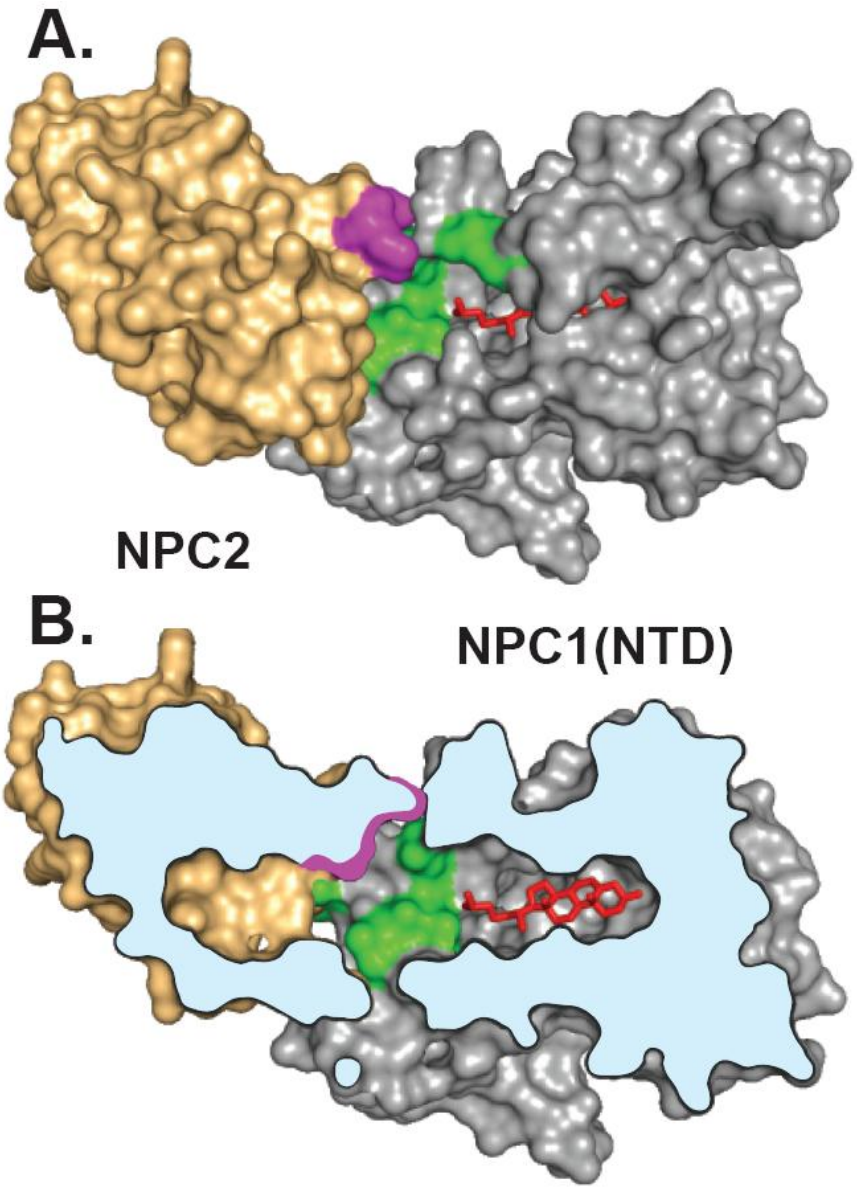

(Spatial alignment of NPC2 and NPC1(NTD) by Hyock Kwon)

DISCUSSION

In the current studies, we used alanine-scanning mutagenesis to identify residues in NPC2 that are important for cholesterol binding and for cholesterol transfer to or from NPC1(NTD). When the crucial residues are mapped to the published structure of NPC2 (Xu et al., 2007), they reveal that the binding-defective mutations cluster around the sterol-binding pocket. Three of the mutant proteins bound cholesterol normally, but failed to catalyze the transfer of cholesterol from NPC1(NTD) to PC liposomes. These three sites were all on the surface of the protein in a patch that is adjacent to the opening of the sterol-binding pocket.

We previously performed a similar alanine-scanning mutagenesis study of NPC1(NTD) (Kwon et al., 2009). In that study, we identified 11 amino acids whose replacement disrupted transfer without disrupting cholesterol binding. These residues clustered in a surface patch of NPC1(NTD) surrounding the helices that must be moved aside in order for cholesterol to enter the binding pocket. The finding that transfer mutants in both proteins cluster in surface patches raises the possibility that these two patches must interact in order for NPC2 to open the binding pocket of NPC1(NTD) so that cholesterol can move between the two proteins. Figure 2-7 shows a model illustrating one way in which these two proteins could interact. The hypothesis of direct interaction between NPC2 and NPC1(NTD) is by no means proven. So far we have been unable to demonstrate a stable physical complex between these two proteins with or without cholesterol in the binding pockets.

The model for direct cholesterol transfer between NPC2 and NPC1(NTD) is formally analogous to the proposed model for substrate channeling between two sequential enzymes in a biochemical pathway (Anderson, 1999). A well studied example of substrate channeling is the transfer of β-aspartyl phosphate between aspartokinase-homoserine dehydrogenase I and aspartate semialdehyde dehydrogenase (James and Viola, 2002). So far, the evidence for such

channeling is kinetic, much like the current evidence for cholesterol transfer in the NPC2/NPC1(NTD) system. Figure 2-6 demonstrates that excess unlabeled cholesterol does not compete for the transfer of [^{3}H]cholesterol prebound to NPC2 to NPC1(NTD) at a 3 minute time point. However, with increasing time, the free cholesterol does compete, most likely owing to dissociation followed by re-association of cholesterol from the NPC proteins. This is highly suggestive of a channeling process. To our knowledge, direct complexes between two different enzymes in substrate channeling have not been demonstrated. On the other hand, in the case of tryptophan synthase in which two sequential enzymes are linked together in a $\alpha_2ß_2$ tetrameric complex, crystallographic studies document intersections between the two active sites (Anderson, 1999).

In the case of channeling systems not involving stable heterodimeric complexes, it is likely that the interactions are transient, and additional methods, such as chemical crosslinking, may be necessary to freeze the contacts so as to permit a direct demonstration of relevant interactions. Initial efforts to use nonspecific crosslinkers to detect interaction between NPC2 and NPC1(NTD) have so far been unsuccessful. We have also been unsuccessful in using several detection methods such as gel filtration, Biacore, and AlphaScreen. Transfer-defective mutants like NPC2(V81D) provide negative controls that allow us to study only the physiologically relevant interactions.

The transfer of cholesterol from NPC2 to NPC1(NTD) has a special functional relevance in light of the near-absolute insolubility of cholesterol in water. Our model envisions that NPC2 binds cholesterol the instant that it is released from LDL, either as the free sterol or after cleavage of cholesteryl esters by lysosomal acid lipase. This binding would prevent cholesterol from crystallizing in the lysosomal lumen. According to the model, NPC2 can transfer its bound

cholesterol to NPC1(NTD) directly, thus avoiding the necessity for the insoluble cholesterol to transit the water phase. We have named this process a "hydrophobic handoff." Additional studies will be needed to test and validate this model. The transfer mutants described in this chapter should facilitate this validation.

Material from Chapter 2 was originally published in Cell Metabolism. Wang ML, Motamed M, Infante RE, Abi-Mosleh L, Kwon HJ, Brown MS, Goldstein JL. Identification of Surface Residues on Niemann-Pick C2 (NPC2) Essential for Hydrophobic Handoff of Cholesterol to NPC1 in Lysosomes. *Cell Metab.* 2010 Aug 4;12(2):166-73.

CHAPTER THREE

IDENTIFICATION OF LUMINAL LOOP 1 OF SCAP AS THE STEROL SENSOR THAT MAINTAINS CHOLESTEROL HOMEOSTASIS

SUMMARY

Cellular cholesterol homeostasis is maintained by Scap, an endoplasmic reticulum (ER) protein with eight predicted transmembrane helices. In cholesterol-depleted cells, Scap transports Sterol Regulatory Element-binding Proteins (SREBPs) to the Golgi where the active fragment of SREBP is liberated by proteases so that it can activate genes for cholesterol synthesis. When ER cholesterol increases, Scap binds cholesterol, and this interaction changes the conformation of cytosolic Loop 6, which contains the binding site for COPII proteins. The altered conformation precludes COPII binding, abrogating movement to the Golgi. Consequently, cholesterol synthesis declines. Here, we identify the cholesterol-binding site on Scap as Loop 1, a 245-amino acid sequence that

projects into the ER lumen. Recombinant Loop 1 binds sterols with a specificity identical to that of the entire Scap membrane domain. When tyrosine-234 in Loop 1 is mutated to alanine, Loop 6 assumes the cholesterol-bound conformation, even in sterol-depleted cells. As a result, full length Scap(Y234A) cannot mediate SREBP processing in transfected cells. These results indicate that luminal Loop 1 of Scap controls the conformation of cytosolic Loop 6, thereby determining whether cells produce cholesterol.

INTRODUCTION

The endoplasmic reticulum (ER) protein Scap is unique in nature because it serves as a cholesterol sensor that assures the proper amount of cholesterol in membranes of animal cells (Radhakrishnan et al., 2007; Sun et al., 2007). The function of Scap derives from its ability to mediate the regulated transport of Sterol Regulatory Element-binding Proteins (SREBPs) from ER to Golgi. SREBPs are a family of three transcription factors that have the capacity to activate all of the genes necessary to produce cholesterol, fatty acids, and triglycerides (Horton et al., 2002). The SREBPs are synthesized as intrinsic transmembrane proteins of the ER. Immediately after their synthesis, the SREBPs bind to Scap, which serves as the nidus for incorporation into COPII-coated vesicles, which bud from the ER and travel to the Golgi. There the SREBPs are processed sequentially by two proteases, thereby releasing the active transcriptional fragments which travel to the nucleus. When cholesterol accumulates in ER membranes, Scap binds the cholesterol and undergoes a conformational change which causes it to bind to Insig, an ER resident protein (Goldstein et al., 2006). As a result of the conformational change and its stabilization by Insig (Gong et al., 2006), the Scap•SREBP complex is no longer incorporated into budding vesicles, and the active fragment cannot reach the nucleus. As a result, synthesis of cholesterol and fatty acids declines.

The 1276 amino acids of Scap can be divided into two functional regions (see Fig. 3-1). The COOH-terminal domain of ~540 amino acids extends into the cytosol. It contains four to seven WD repeat sequences that mediate its binding to SREBPs. The NH_2-terminal region of ~735 amino acids is the membrane attachment domain. It contains eight α-helices separated by hydrophilic loops (Nohturfft et al., 1998). Three of the loops (Loops 1, 6, and 7) are long

enough to have significant structure. Helices 2-6 contain the Insig binding site (Yang et al., 2002; Yabe et al., 2002b). Loop 6, which faces the cytosol, contains the hexapeptide sequence MELADL which serves as the binding site for the COPII proteins that cluster the Scap•SREBP complex into COPII-coated vesicles that bud from ER membranes (Sun et al., 2005; Sun et al., 2007). When the cholesterol content of ER membranes exceeds a sharp threshold of 4-5% of total lipids, the cholesterol binds to the membrane region of Scap (Radhakrishnan et al., 2008), and this elicits a conformational change in Loop 6 that can be monitored by a protease protection assay (Brown et al., 2002). The change is reflected by the exposure of a novel arginine (Arg505) to cleavage by trypsin (Fig. 3-1).

The cholesterol-induced conformational change in Loop 6 causes the MELADL sequence to become inaccessible to COPII proteins, thereby precluding transport to the Golgi (Sun et al., 2007). Although the conformational change does not require Insig, binding to Insig stabilizes the inactive conformation, thereby lowering the threshold for cholesterol (Radhakrishnan et al., 2008).

Our previous cholesterol-binding studies were performed with a recombinant form of Scap that contained the entire membrane attachment domain (TM1-8) (Radhakrishnan et al., 2004; Radhakrishnan et al., 2007). Within this domain the precise site of cholesterol binding was not established. In the current study, we localize the cholesterol-binding site to Scap Loop 1, which faces the ER lumen. We show that a point mutation in Loop 1 elicits the same conformational change in Loop 6 that is created by cholesterol binding. As a result, Scap with this point mutation cannot move from ER to Golgi, even in cholesterol-depleted cells. These studies implicate an interplay between luminal Loop 1 and cytosolic Loop 6 of Scap as a control mechanism for the regulation of cholesterol metabolism in animal cells.

EXPERIMENTAL PROCEDURES

Reagents – We obtained [1,2,6,7-^{3}H]cholesterol (100 Ci/mmol) and [26,27-^{3}H]25-hydroxycholesterol (75 Ci/mmol) from American Radiolabeled Chemicals; 24,25-epoxycholesterol and 24(S)-hydroxycholesterol from Avanti Polar Lipids; all other sterols from Steraloids, Inc.; Nonidet P-40 (NP-40), FuGENE 6, and Complete Protease Inhibitor Cocktail from Roche Applied Sciences; Protease Inhibitor Cocktail Set III and mouse anti-HSV monoclonal antibody from Novagen; trypsin (type I from bovine pancreas), monoclonal anti-Green Fluorescent Protein (GFP), anti-c-Myc Affinity Gel, c-Myc peptide and cycloheximide from Sigma; peptide N-glycosidase (PNGase F) from New England Biolabs; Fos-choline 13 from Anatrace; Ni-NTA agarose beads from Qiagen; cyclodextrins from Trappsol; mouse anti-His monoclonal antibody, Superdex 200 10/300 GL, Mono Q 5/50 GL, and HisTrap HP columns from GE Healthcare Biosciences; Gel Filtration Standard from Bio-Rad; rat anti-*Drosophila* hsc72 (BiP) polyclonal antibody from Babraham Institute, Cambridge UK (Cat. No. BT-GB-1435); phRL-TK (encoding *Renilla luciferase* gene) and Dual-Luciferase Reporter Assay System from Promega; and bovine serum albumin (Cat. No. 23209) from Thermo Scientific. Complexes of methyl-β-cyclodextrin with cholesterol were prepared at a stock concentration of 2.5 mM (Brown et al., 2002). Newborn calf lipoprotein-deficient serum (d>1.215 g/ml) was prepared by ultracentrifugation (Goldstein et al., 1983). Solutions of compactin and sodium mevalonate were prepared as previously described (Brown et al., 1978; Kita et al., 1980). A stock solution of 10 mM sodium oleate-bovine serum albumin in 0.15 M NaCl (final pH 7.6) was prepared as previously described (Hannah et al., 2001). IgG-4H4, a mouse monoclonal antibody against hamster Scap (amino acids 1-767) (Ikeda et al., 2009) and IgG-9E10, a mouse monoclonal

antibody against c-Myc (Yabe et al., 2002a), were previously described in the indicated reference.

Buffers – Buffer A contained 50 mM Tris-chloride (pH 7.4), 150 mM NaCl, 1 mM dithiothreitol (DTT), and 0.005% (w/v) sodium azide. Buffer B contained 50 mM Tris-chloride (pH 7.4), 1 mM DTT, and 0.005% sodium azide. Buffer C contained 50 mM Tris-chloride (pH 7.4), 150 mM NaCl, and 0.004% NP-40. Buffer D contained 50 mM Tris-chloride (pH 7.4) and 150 mM NaCl. Buffer E contained 50 mM Tris-chloride (pH 7.5), 150 mM NaCl, 1 mM DTT, and 25 mM phosphocholine chloride. Buffer F contained 10 mM HEPES (pH 7.4), 10 mM KCl, 1.5 mM $MgCl_2$, 5 mM sodium EDTA, 5 mM sodium EGTA, and 250 mM sucrose. Buffer G contained 50 mM Tris-chloride (pH 7.4), 135 mM NaCl, 10 mM KCl, and 0.1% NP-40, and 1% (v/v) Protease Inhibitor Cocktail Set III.

Culture Medium – Medium A contained a 1:1 mixture of Ham's F-12 and Dulbecco's modified Eagle's medium supplemented with 100 units/ml penicillin and 100 μg/ml streptomycin sulfate. Medium B contained medium A supplemented with 5% newborn calf lipoprotein-deficient serum, 50 μM sodium mevalonate, and 50 μM compactin, and 1% (w/v) hydroxypropyl-β-cyclodextrin. Medium C contained medium A supplemented with 5% newborn calf lipoprotein-deficient serum, 50 μM sodium mevalonate, and 50 μM compactin. Medium D contained Dulbecco's modified Eagle's medium, low glucose (1000 mg/l) supplemented with 10% FCS and 100 units/ml penicillin and 100 μg/ml streptomycin sulfate.

Plasmids – The pFastBacHTa expression vector encoding amino acids 1-767 of hamster Scap, referred to as His_{10}-Scap(TM1-8) (Radhakrishnan et al., 2004), was modified by site-directed mutagenesis (QuikChange II XL kit, Stratagene) to generate a recombinant baculovirus designated $pHis_6$-Scap(Loop1). $pHis_6$-Scap(Loop1) encodes, in sequential order from the NH_2-

terminus, the signal sequence from honeybee mellitin (Tessier et al., 1991), an epitope tag consisting of 6 histidines, a TEV protease cleavage site (Kapust et al., 2002), and luminal Loop 1 of Scap (amino acids 46-269).

The following recombinant expression plasmids have been described: pCMV-Scap, encoding WT hamster Scap under control of cytomegalovirus (CMV) promoter (Sakai et al., 1997); pTK-Scap, encoding WT hamster Scap under control of thymidine kinase (TK) promoter; pGFP-Scap, encoding GFP fused to WT hamster Scap under control of the CMV promoter (Nohturfft et al., 2000); pTK-HSV-BP2, encoding WT HSV-tagged human SREBP-2 under control of the TK promoter (Feramisco et al., 2005); pTK-Insig-1-Myc, encoding WT human Insig-1 followed by six tandem copies of c-Myc epitope tag under control of TK promoter (Gong et al., 2006); pCMV-Insig1-Myc, encoding human Insig-1 followed by 6 tandem copies of a c-Myc epitope tag (Yabe et al., 2002b); and pSRE-Luc, encoding three tandem copies of Repeat 2 + Repeat 3 of the human LDL receptor promoter, the adenovirus E1b TATA box, and the *Firefly luciferase* gene (Hua et al., 1996). Point mutations in the above Scap plasmids were produced by site-directed mutagenesis. The coding regions of all mutated plasmids were sequenced.

Purification of His-Tagged Scap(Loop1) from Sf9 Cells – On day 0, 1-liter cultures of Sf9 cells (5 x 10^5 cells/ml) in Sf-900 II SFM insect medium (Invitrogen) were set up at 27°C. On day 1, cells were infected with His_6-Scap(Loop1) baculovirus. On day 3, cells were harvested and washed once with phosphate-buffered saline (PBS). The cells were then flash-frozen with liquid nitrogen and stored at -80°C. Each pellet was resuspended in 10 pellet volumes of buffer A containing 1% (w/v) Fos-choline 13 and one Complete Protease Inhibitor Cocktail tablet per 50 ml, rotated for 1 h at 4°C, and centrifuged at 10^5x*g* for 1 h at 4°C. The resulting supernatant was loaded onto a 1-ml or 5-ml HisTrap HP column equilibrated with 10 column volumes of

buffer A containing 0.1% Fos-choline 13, then washed sequentially with 10 column volumes of buffer A containing 0.1% Fos-choline 13 and 5 mM imidazole, followed by 25 mM imidazole. The protein was then eluted with 5 column volumes of the above buffer containing 250 mM imidazole. Protein rich fractions containing His_6-Scap(Loop1) were combined and concentrated with a Millipore Centrifugal Filter Unit (10 kDa MWCO) to 1 ml, and then diluted 40-fold in buffer B containing 0.1% Fos-choline 13. The resulting solution was applied to a 1-ml Mono Q column, and the protein was eluted with the above buffer containing 50 mM NaCl. The peak fractions containing His_6-Scap(Loop1) were combined, concentrated to 0.5 ml with a Millipore Centrifugal Filter Unit (10 kDa MWCO), and then applied to a Superdex 200 10/300 GL column. His_6-Scap(Loop1) was eluted with buffer B containing 0.1% Fos-choline 13 between 12.5 ml and 14.5 ml, after which these fractions were combined, stored at 4°C, and used for assays within 2 days.

[^{3}H]Cholesterol-binding Assay – All operations were carried out at room temperature. Binding reactions were set up in microcentrifuge tubes. Each reaction, in a final volume of 100 μl of buffer C with 0.004% NP-40, contained 5 pmol (150 ng) of purified His_6-Scap(Loop1) (delivered in 1 μl of buffer B containing 0.1% Fos-choline 13; final concentration in assay, 0.001%), and the indicated concentration of [^{3}H]sterol (delivered in 2 μl ethanol) in the absence or presence of competitor sterol (delivered in 1 μl ethanol). After incubation for 4 h at room temperature, each reaction was loaded onto a column packed with 0.3 ml of Ni-NTA agarose beads preequilibrated with 2 ml of buffer D. The columns were washed with 5 ml of buffer D, and then eluted with 1 ml of the same buffer containing 250 mM imidazole. Aliquots of the eluate (0.7 ml) were assayed for radioactivity in a liquid scintillation counter.

[^{3}H]Cholesterol Dissociation Assay – [^{3}H]Cholesterol was prebound to His_6-Scap(Loop1) under standard assay conditions with 150 nM [^{3}H]cholesterol (see above) except that the assay was scaled up 40-fold. After incubation for 4 h at room temperature, the protein-bound [^{3}H]cholesterol was eluted from the Ni-NTA agarose beads in 1 ml and then diluted to a final volume of 6 ml with buffer A containing 0.1% Fos-choline 13. For the dissociation assay, the 6-ml mixture containing [^{3}H]cholesterol bound to His_6-Scap(Loop1) was divided into two aliquots of 3 ml, each of which received an addition of 24 ml of buffer C in the absence or presence of 11 μM unlabeled cholesterol. After incubation at room temperature for the indicated time, a 1-ml aliquot from each of the 27-ml sample was transferred to a tube containing 600 μl of Ni-NTA-agarose beads. After incubation for 3 min at 4°C, the beads were centrifuged at 800x*g* for 1 min at room temperature, after which the supernatant was assayed for radioactivity.

Cell Culture and Transfection – SRD-13A cells, a Scap-deficient cell line derived from CHO-7 cells (Rawson et al., 1999), were grown in monolayer at 37°C in 8-9% CO_2 in medium A supplemented with 5% FCS, 1 mM sodium mevalonate, 20 mM sodium oleate-albumin, and 5 μg/ml cholesterol. SV589 cells, a line of SV-40 immortalized human fibroblasts (Yamamoto et al., 1984), were grown in monolayer at 37°C in 5% CO_2 in medium D. Hamster CHO-K1 cells were grown in monolayer at 37°C and 8-9% CO_2 in medium A supplemented with 5% FCS.

Trypsin Cleavage Assay of Scap – This assay was carried out as previously described by Brown, et al. (2002) with modifications in the culture and transfection conditions. On day 0, SRD-13A cells were set up for experiments in 10 ml of medium A containing 5% FCS at a density of $8x10^5$ cells per 100-mm dish. On day 2, cells were transfected with 1 μg of full length WT pCMV-Scap or its mutant Y234A version in 7 ml of medium A supplemented with 5% FCS; FuGENE 6 was used as the transfection agent. On day 3, the cells were washed once with PBS,

harvested for preparation of membranes, and subjected to the trypsin cleavage assay (Brown et al., 2002).

Assay for Scap•Insig Complex – SRD-13A cells were set up for experiments as described above under "Trypsin Cleavage Assay of Scap" except that the cells were plated in 60-mm dishes at a density of $3x10^5$ cells per dish. On day 2, the cells were transfected with 0.1 μg pCMV-Insig1-Myc and 1 μg of either full length WT pCMV-Scap or its mutant Y234A version. On day 3, the cells were switched to cyclodextrin-containing medium B. After incubation at 37°C for 1 h, cells were washed twice with PBS and switched to medium C in the absence or presence of either 30 μM cholesterol complexed with methyl-β-cyclodextrin or 1 μg/ml 25-hydroxycholesterol (delivered in ethanol, final concentration of 0.1%). After incubation for 4 h, cells were washed twice with PBS and harvested. The pellets from three 60-mm dishes of transfected SRD-13A cells were solubilized in 1 ml of NP-40-containing buffer G, passed through a 22.5-gauge needle 15 times and rotated for 1.5 h at 4°C. All subsequent operations were carried out at 4°C unless otherwise stated. The cell extracts were clarified by centrifugation at 10^5x*g* for 30 min. Anti-Myc beads (50 μl) were added to the supernatant, followed by rotation for 16 h and centrifugation at 2000x*g* for 1 min. The pelleted beads containing the immune complexes were washed on the rotator with 1 ml of buffer G for 30 min, followed by three additional washes in buffer G for 10 min each. The washed beads were eluted in 100 μl buffer G with 0.25 mg/ml c-Myc peptides by rotating for 1 h at room temperature. After centrifugation at 2000x*g* for 1 min, the supernatant was subjected to immunoblot analysis.

SREBP-2 Processing in Cultured Cells – SRD-13 cells were set up for experiments as described in the legend to Fig. 3-7A. After transfection and incubation with sterols, nuclear and

membrane fractions were prepared as previously described (Feramisco et al., 2005) and then subjected to immunoblot analysis.

Immunoblot Analysis – Samples for immunoblotting were resolved with to 10% or 13% SDS/PAGE or electrophoresis on 12% Tris-tricine gels, after which the proteins were transferred to nitrocellulose filters that were incubated with the following primary antibodies: 1 μg/ml mouse monoclonal anti-His, 1:500 dilution of a rat antiserum directed against *Drosophila* hsc72 (BiP), 1 μg/ml mouse monoclonal anti-Myc IgG-9E10, or 5 μg/ml mouse monoclonal anti-Scap IgG-4H4. Bound antibodies were visualized by chemiluminescence (SuperSignal West Pico Chemiluminescent Substrate, Thermo Scientific) using a 1:5000 dilution of anti-mouse IgG (Jackson ImmunoResearch Laboratories, Inc.) or anti-rat IgG (GE Healthcare) conjugated to horseradish peroxidase. The films were exposed to Phoenix Research Products Blue X-ray Film (F-BX810) at room temperature.

RESULTS

Fig. 3-1 shows the sequence and the predicted topology of the membrane domain of Scap as deduced from previous studies (Nohturfft et al., 1998). This segment has 8 predicted transmembrane helices and 3 loops that are large enough to have secondary structure. Loop 1 comprises 245 amino acids and faces the lumen. It contains a site for *N*-linked glycosylation near its C-terminus. Loop 6, which faces the cytosol, was shown previously to contain the sequence MELADL, which is the binding site for COPII proteins that carry the Scap•SREBP complex from ER to Golgi (Sun et al., 2005; Sun et al., 2007). Loop 7, which faces the lumen, contains an epitope that allows immunodetection of a tryptic fragment that changes in response to a sterol-induced conformational change in the structure of Loop 6 (Brown et al., 2002; Sun et al., 2007).

We prepared a baculovirus encoding nearly the entire Loop 1 (residues 46-269) preceeded by a cassette comprised of the signal sequence from honeybee mellitin followed by 6 histidines and a TEV protease cleavage site. After introduction into insect cells, the cells produced Loop 1 as a membrane-attached protein (Fig. 3-2A, *lanes 1, 2*). No detectable amounts of Loop 1 were secreted into the medium. Membrane-bound Loop 1 showed two bands upon SDS-PAGE. NH_2-terminal sequencing by Edman degradation revealed that the upper band represents protein that retains the signal sequence because it has not been cleaved by signal peptidase. The lower band contains protein that was processed by signal peptidase. Treatment with TEV protease reduced both proteins to a single band (data not shown). Both forms of the protein could be solubilized from the membrane by treatment with a detergent (Fos-choline 13) (Fig. 3-2A, *lanes 3, 4*), but neither one was released by treatment with Na_2CO_3 at pH 11 (Fig. 3-2A, *lanes 5, 6*), indicating that Loop 1 is attached to the membrane by hydrophobic forces. The detergent-solubilized protein was purified by sequential chromatography on a nickel agarose column and an ion exchange column, followed by gel filtration. Upon gel filtration in 0.1% Fos-choline 13, the protein had an apparent molecular mass of 125 kDa (Fig. 3-2B), consistent with a tetramer. Circular dichroism indicated a largely helical structure (Fig. 3-2C).

Sterol-binding studies were performed with preparations of purified Scap Loop 1 that contained molecules with and without the signal sequence. To measure cholesterol binding, we incubated the recombinant protein with [^{3}H]cholesterol in buffer containing 0.004% NP-40 and 0.001% Fos-choline 13. The mixture was applied to a nickel agarose column that was washed without detergent, and the protein-bound [^{3}H]cholesterol was eluted with 250 mM imidazole in detergent-free buffer and quantified by scintillation counting. As shown in Fig. 3-3, the recombinant Loop1 bound [^{3}H]cholesterol with saturation kinetics (calculated K_d = 67 nM),

which is comparable to the apparent K_d of 50-100 nM when the binding studies were performed with the entire membrane attachment domain (TM1-8) (Radhakrishnan et al., 2004). The rate of dissociation of previously bound [^{3}H]cholesterol from Loop 1, as measured in the presence of an excess of unlabeled cholesterol, was similar to that previously shown for Scap(TM1-8), i.e., half-time of dissociation of ~10 min (Fig. 3-4 and see Fig. 4 from Radhakrishnan, *et al.*) (Radhakrishnan et al., 2004). Moreover, like the entire membrane domain of Scap, Loop 1 did not bind [^{3}H]25-hydroxycholesterol with high affinity (Fig. 3-3B).

To analyze the sterol specificity of Loop 1 binding, we performed competition studies with various unlabeled sterols. Androstenol and desmosterol competed as well as cholesterol for [^{3}H]cholesterol binding, whereas epicholesterol, lanosterol and 25-hydroxycholesterol did not compete (Fig. 3-5A). Fig. 3-5B compares the ability of various sterols at 1.5 μM to compete for [^{3}H]cholesterol binding to Loop 1. For comparative purposes, Fig. 3-5C is reproduced from Fig. 3D of Radhakrishnan, *et al*, (2007), who studied sterol competition for [^{3}H]cholesterol binding to the entire transmembrane region of Scap, designated Scap(TM1-8). The sterols are grouped into effective competitors (*shown in red*), partial competitors (*shown in blue*), and non-competitors (*shown in black*). The sterol specificity of Loop 1 coincides precisely with that of the entire transmembrane domain.

We next carried out alanine scan mutagenesis of Loop 1 to identify functional residues. Single residues or clusters of 2 or 3 contiguous residues were changed to alanine in a *Herpes simplex* TK vector that encodes full length Scap. The mutant plasmids were introduced into hamster SRD-13A cells, a mutant CHO cell line that lacks Scap (Rawson et al., 1999), together with plasmids encoding firefly luciferase under control of an SRE-containing promoter and

Insig-1 under control of the TK promoter. To control for transfection efficiency, we included a plasmid encoding *Renilla* luciferase under control of the TK promoter. The cells were depleted of cholesterol by incubation with hydroxypropyl-β-cyclodextrin, and some of the cells were repleted by addition of cholesterol complexed with methyl-β-cyclodextrin. The cells were harvested, and the ratio of firefly to *Renilla* luciferase was measured. In cells that received no Scap, there was little firefly luciferase activity (Fig. 3-6A). WT Scap led to high luciferase activity that was reduced by 80% in the presence of cholesterol. Several of the mutant plasmids showed no luciferase activity in the absence of cholesterol (indicated by red asterisks in Fig. 3-6A). We concluded that these mutations impaired the ability of Scap to carry SREBPs to the Golgi region.

To deconvolute the cluster mutations that appeared to abolish Scap activity, we prepared additional plasmids in which each of the residues in each cluster was changed individually to alanine (Fig. 3-6B). These data revealed two single amino acid substitutions that abolished Scap activity. These were V98A and Y234A. We chose the Y234A mutant for further study.

To visualize directly the lack of movement of Scap(Y234A) to the Golgi, we introduced the Y234A mutation into a plasmid encoding a fusion protein between Scap and green fluorescent protein (GFP) (Fig. 3-7). Cells were depleted of sterols and then fixed and permeabilized for fluorescence microscopy. Scap was visualized by its GFP tag. The Golgi complex was visualized by incubation with an antibody directed against Golgi protein GM130 followed by an anti-immunoglobulin coupled to a red Alexa dye. Nuclei were stained with Hoechst dye (blue). Under these conditions, WT Scap-GFP was concentrated in the Golgi where it co-localized with GM130 (*upper panels,* Fig. 3-7). In contrast, the vast majority of Scap(Y234A) was found in a lacy pattern corresponding to ER, and there was no specific localization to the Golgi (*bottom*

panels, Fig. 3-7). The images shown in Fig. 3-7 are representative of multiple transfected cells that were individually examined (n=79 WT and n=70 mutant).

To confirm that the Y234A mutation abolishes the ability of Scap to facilitate SREBP processing, we transfected plasmids encoding WT or Y234A mutant Scap into Scap-deficient SRD-13A cells (Fig. 3-8A). Some of the cells also received a plasmid encoding Myc-tagged Insig-1. The cells were depleted of sterols, and some were repleted with cholesterol or 25-HC. Nuclear extracts and membrane pellets were isolated and subjected to SDS/PAGE. In the absence of co-transfection with Insig-1, overexpression of WT Scap caused the appearance of the nuclear fragment of SREBP-2 (*lane 2*), and there was minimal reduction when cholesterol or 25-HC was added (*lanes 3* and *4*). When Insig-1 was overexpressed together with WT Scap, the nuclear fragment of SREBP-2 was seen in sterol-depleted cells (*lane 5*), and the fragment disappeared when cholesterol or 25-HC were present (*lanes 6* and *7*). When cells expressed Scap(Y234A), nuclear SREBP-2 was barely detectable in the absence or presence of sterols, and Insig-1 had no further inhibitory effect (*lanes 8-13*). Immunoblotting with anti-Scap confirmed the equal expression of WT and Y234A mutant Scap after transfection (*lanes 2-13*, Scap immunoblot).

To learn the reason for the defective behavior of Scap(Y234A), we introduced the mutation into a baculovirus encoding His-tagged Scap(Loop1), and we purified the mutant loop together with WT Loop 1 as described above. Both mutant and WT Loop 1 bound [^{3}H]cholesterol with similar affinity (Fig. 3-8B). Fig. 3-8C shows the trypsin cleavage assay that we used previously to demonstrate a sterol-induced conformational change in Loop 6 of Scap (Brown et al., 2002; Sun et al., 2007) (see Fig. 3-1). Cells were transfected with plasmids encoding full-length WT Scap or the Y234A mutant. A 20,000x*g* pellet of sealed vesicles was isolated and incubated with

or without cholesterol complexed to methyl-β-cyclodextrin. The membranes were then treated with trypsin, after which the proteins were subjected to Tris-tricine gel electrophoresis and blotted with an antibody against an epitope in Loop 7 that faces the lumen and is thus protected from trypsin (see Fig. 3-1). In sterol-depleted membranes, trypsin cleaves Loop 6 at arginine 496 and arginines 747-750, which produces a fragment of 250 amino acids that corresponds to the band seen in Fig. 3-8C, *lane 1*. After incubation with cholesterol, arginines 503 and 505 become exposed to trypsin. Cleavage at these sites produces a fragment of ~241 amino acids, which corresponds to the lower band (*lane 3*). The Y234A mutant of Scap showed substantial amounts of the lower band, even in cholesterol-depleted membranes (*lane 2*). There was a further reduction in the upper band when cholesterol was added (*lane 4*). These data indicate that Loop 6 in the Y234A mutant is largely in the cholesterol-bound conformation even in sterol-depleted membranes.

When Scap is in the cholesterol-bound conformation, the protein binds to Insig, which stabilizes the cholesterol-bound conformation (Yang et al., 2002). Fig. 3-8D shows an experiment designed to determine whether Scap(Y234A) binds to Insig-1 in sterol-depleted cells as determined by an Insig-1 co-immunoprecipitation assay. Scap-deficient SRD-13A cells were co-transfected with plasmids encoding Myc-tagged Insig-1 and either WT Scap or the Y234A mutant. The cells were depleted of cholesterol, and some were repleted with cholesterol or 25-HC. Detergent extracts were prepared, and Insig-1 was precipitated with anti-Myc. After SDS-PAGE, the precipitates were probed with antibodies against Scap and Insig-1. In sterol-depleted cells, WT Scap did not co-precipitate with Insig-1 (Fig. 3-8D, *lane 1*). Addition of cholesterol (*lane 2*) or 25-HC (*lane 3*) caused Scap to be co-precipitated. In contrast, Scap(Y234A) was co-precipitated with Insig-1 even in the absence of sterol (*lane 4*), and the amount co-precipitated

increased when 25-HC was added (*lane 6*). In the immunoblots in this experiment, we noted that Scap showed two bands. We believe that the upper band represents an SDS-resistant dimer that forms when Scap has been incubated in detergents for prolonged periods, as required for the co-immunoprecipitation experiment. Insig-1 also appears as a doublet owing to the presence of two initiator methionines (Yang et al., 2002).

FIGURE 3-1. Topology model of the membrane region of hamster Scap, showing its three functional domains.

The cholesterol-binding domain is localized to luminal Loop 1; the three hydrophobic patches in its amino acid sequence are shaded in yellow, and the *N*-linked glycosylation site is denoted by the red box. The Insig-binding domain is localized to transmembrane helices 2-6, shown by the blue bracket. The COPII-binding site is localized to the MELADL sequence in Loop 6, shaded in red. Amino acids 496-747/750 (shaded in purple) correspond to the trypsin-resistant fragment generated by a sterol-regulated conformational change in Scap.

FIGURE 3-1

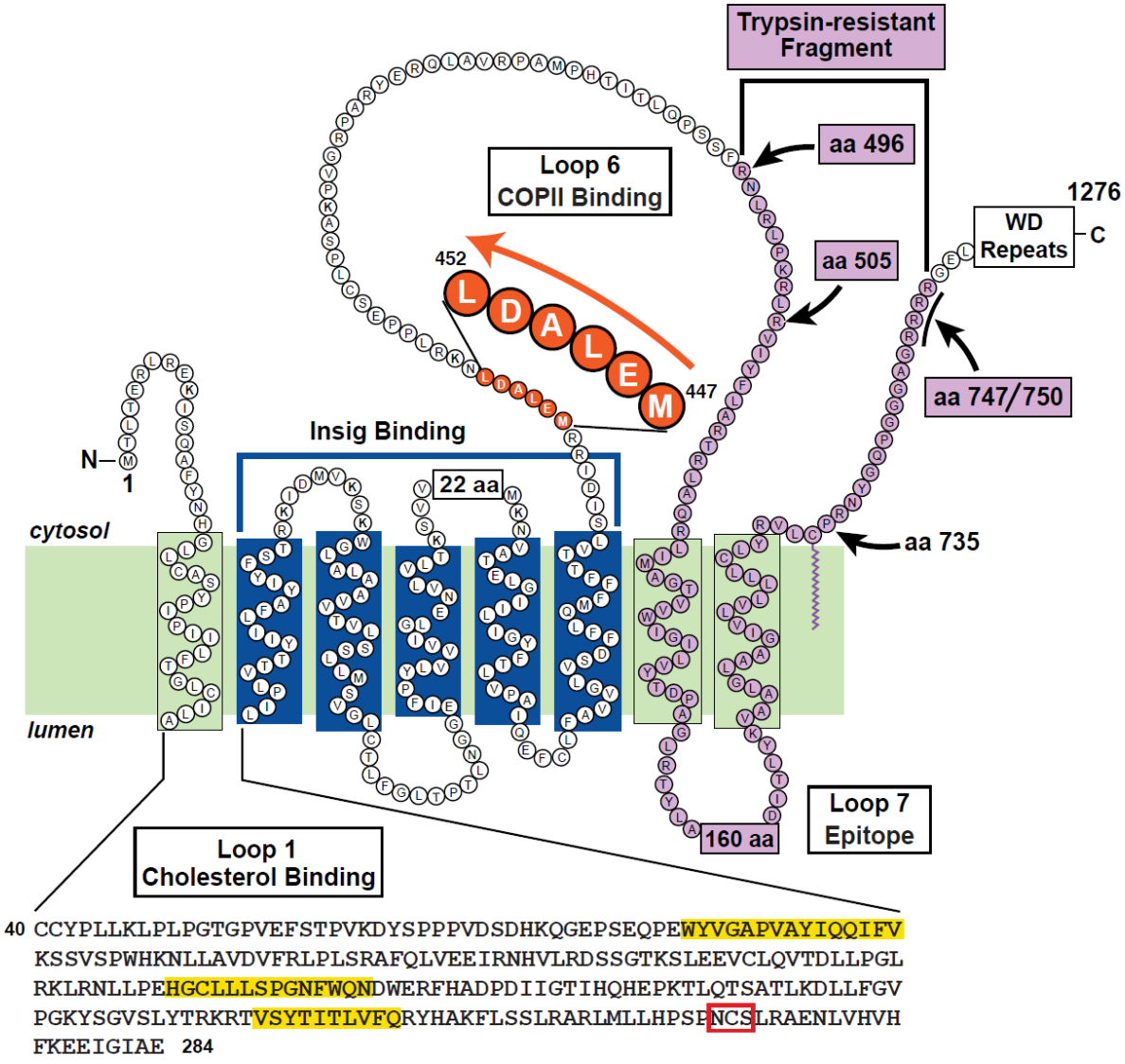
Trypsin-resistant Fragment
aa 496
Loop 6 COPII Binding
1276
WD Repeats
C
aa 505
452
L D A L E M
447
aa 747/750
Insig Binding
N
1
22 aa
cytosol
aa 735
lumen
160 aa
Loop 7 Epitope
Loop 1 Cholesterol Binding
40 CCYPLLKLPLPGTGPVEFSTPVKDYSPPPVDSDHKQGEPSEQPEWYVGAPVAYIQQIFV
KSSVSPWHKNLLAVDVFRLPLSRAFQLVEEIRNHVLRDSSGTKSLEEVCLQVTDLLPGL
RKLRNLLPEHGCLLLSPGNFWQNDWERFHADPDIIGTIHQHEPKTLQTSATLKDLLFGV
PGKYSGVSLYTRKRTVSYTITLVFQRYHAKFLSSLRARLMLLHPSPNCSLRAENLVHVH
FKEEIGIAE 284

FIGURE 3-2. Biochemical properties of His_6-Scap(Loop1).

A, membrane attachment. Aliquots of baculovirus-infected Sf9 cell pellets (representing ~ $2x10^5$ cells) were each homogenized in 0.5 ml of one of the following buffers: 50 mM Tris-chloride (pH 7.4) and 100 mM NaCl (*lanes 1, 2*); buffer A with 1% Fos-choline 13 (lanes 3, 4); or 100 mM sodium carbonate at pH 11 (*lanes 5, 6*). After rotating for 2 h at 4°C, the samples were centrifuged at 10^5x*g* for 30 min at 4°C, after which the resulting pellets were solubilized in 0.5 ml of 10 mM Tris at pH 7.4, 100 mM NaCl, and 1% SDS. Aliquots of the supernatant (S) and pellet (P) were subjected to 13% SDS/PAGE and immunoblot analysis with anti-His (Scap(Loop1)) or anti-BiP. Films were exposed for 8-10 sec. *B*, molecular weight determination. Buffer A containing 0.1% Fos-choline 13 and either gel filtration standards or 125 μg of His_6-Scap(Loop1) were loaded in a final volume of 0.5 ml onto a Superdex 200 10/300 GL column and chromatographed at a flow rate of 0.5 ml/min. Elution volumes for the gel filtration standards and for His_6-Scap(Loop1) were identified by monitoring absorbance at 280 nM and immunoblotting with anti-His, respectively. *C*, circular dichroism spectroscopy. Spectroscopic measurements of 3 μM His_6-Scap(Loop1) in buffer A containing 0.1% Fos-choline 13 were carried out in an Aviv 62DS spectrometer using a 2-mm path length cuvette. The mean of 4 spectra for each curve is shown.

Figure 3-2

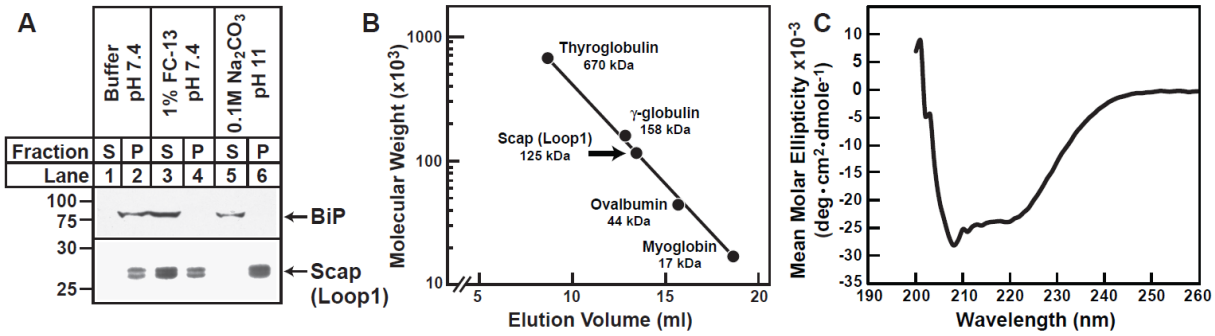
A
Buffer pH 7.4
1% FC-13 pH 7.4
0.1M Na2CO3 pH 11
Fraction S P S P S P
Lane 1 2 3 4 5 6
100
75
30
25
←BiP
←Scap (Loop1)
B
Molecular Weight (x10³)
1000
100
10
Thyroglobulin 670 kDa
γ-globulin 158 kDa
Scap (Loop1) 125 kDa
Ovalbumin 44 kDa
Myoglobin 17 kDa
5 10 15 20
Elution Volume (ml)
C
Mean Molar Ellipticity x10⁻³ (deg·cm²·dmole⁻¹)
10 5 0 -5 -10 -15 -20 -25 -30 -35
190 200 210 220 230 240 250 260
Wavelength (nm)

FIGURE 3-3. [^{3}H]Sterol binding to His$_6$-Scap(Loop1).

Each reaction, in a final volume of 100 μl buffer C with 0.004% NP-40 and 0.001 Foscholine-13, contained 5 pmol of purified His$_6$-SCAP(Loop1), 1 μg bovine serum albumin, and the indicated concentration of either [^{3}H]cholesterol (222 dpm/fmol) or [^{3}H]25-hydroxycholesterol (165 dpm/fmol) in the absence (●) or presence (○) of 10 μM unlabeled sterol as indicated. After 4 h at room temperature, the bound [^{3}H]sterol was measured as described in *Experimental Procedures*. Each data point denotes the mean±SEM of triplicate assays. *A*, total [^{3}H]cholesterol binding without substraction of blank values. *B*, specific [^{3}H]cholesterol or [^{3}H]25-hydroxycholesterol binding after subtraction of blank values determined in the presence of the respective unlabeled sterol at 10 μM (<127 fmol/tube for [^{3}H]cholesterol binding; <30 fmol/tube for [^{3}H]25-hydroxycholesterol binding).

Figure 3-3

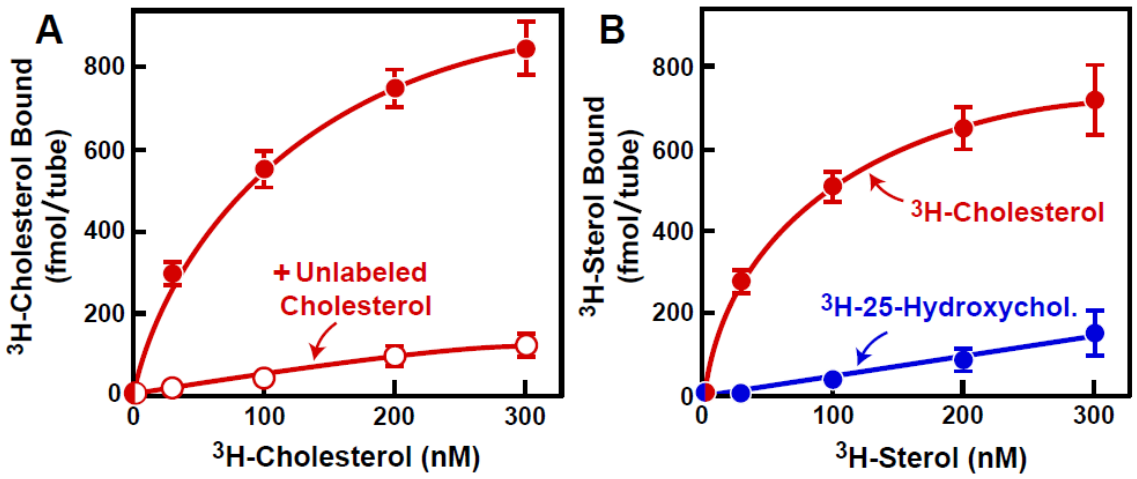

FIGURE 3-4. Association and dissociation of [^{3}H]cholesterol binding to His$_6$-Scap(Loop1). *A*, time course of binding of [^{3}H]cholesterol to His$_6$-Scap(Loop1). Each reaction, in a final volume of 100 μl of buffer C with 0.004% NP-40 and 0.001% Fos-choline 13, contained 5 pmol of His$_6$-Scap(Loop1), 1 μg bovine serum albumin, and 150 nM [^{3}H]cholesterol (222x10^3 dpm/pmol). After incubation for the indicated time at room temperature, bound [^{3}H]cholesterol was determined. Each value is the average of duplicate assays. Blank values obtained in parallel assays of tubes containing no protein (<7 fmol/tube) were subtracted from each data point. *B*, dissociation of previously bound [^{3}H]cholesterol from His$_6$-Scap(Loop1). Dissociation was measured as described in *Experimental Procedures*. Each value is the average of duplicate assays and represents the percentage of [^{3}H]cholesterol remaining bound relative to the zero-time value, which is designated as 100%. The zero-time values were 300 and 230 fmol/tube in the absence and presence of unlabeled cholesterol, respectively.

Figure 3-4

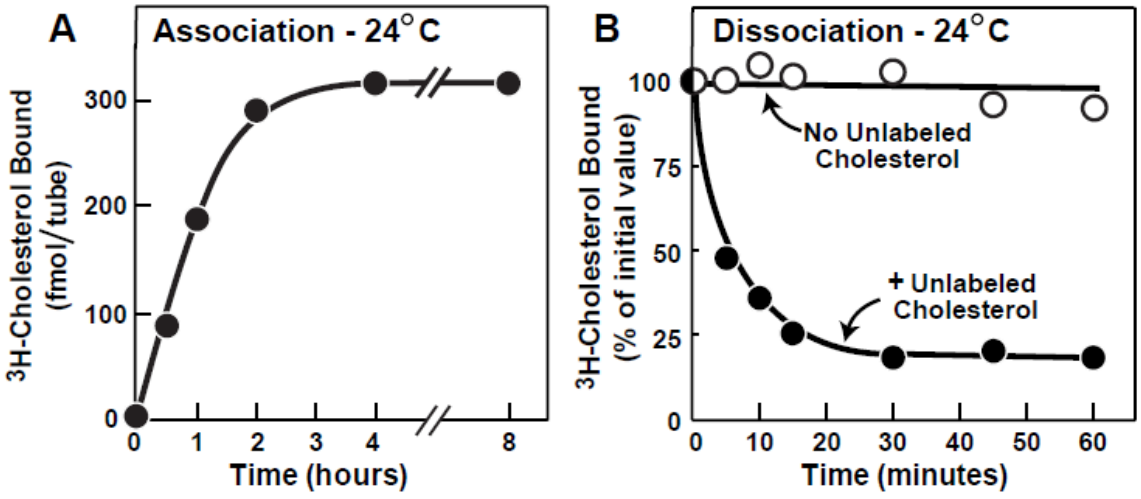

FIGURE 3-5. Comparison of the sterol specificity of [^{3}H]cholesterol binding to Scap(Loop1) and Scap(TM1-8).

A and *B*, competitive binding of unlabeled sterols to His_6-Scap(Loop1). Each reaction, in a final volume of 100 μl of buffer C with 0.004% NP-40 and 0.001% Fos-choline 13, contained 5 pmol of His_6-Scap(Loop1), 1 μg bovine serum albumin, 150 nM [^{3}H]cholesterol (222 dpm/fmol), and either varying concentrations of the indicated unlabeled sterol (*A*) or 1.5 μM of the indicated unlabeled sterol (*B*). After 4 h at room temperature, bound [^{3}H]cholesterol was measured by the Ni-NTA agarose assay as described in *Experimental Procedures*. Each value represents total binding without subtraction of blank values and is the average of duplicate (*A*) or triplicate (*B*) assays. The ‘‘100% of control’’ values, determined in the absence of unlabeled sterols, was 398 fmol/tube and 673 fmol/tube in *A* and *B*, respectively. *C*, competitive binding of unlabeled sterols to His_{10}-Scap(TM1-8). These data are replotted from Fig. 3D of Radhakrishnan et al. (2007). Briefly, each assay tube, in a final volume of 100 μl of buffer E with 0.1% Fos-choline 13, contained 120 nM His_{10}-Scap(TM1-8), 100 nM [^{3}H]cholesterol (120 dpm/fmol), and 5 μM of the indicated sterol. After 4 h at room temperature, the amount of bound [^{3}H]cholesterol was determined by the Ni-NTA agarose assay. The “100% of control” values, determined in the absence of unlabeled sterols, ranged from 209-263 fmol/tube. No blank values were subtracted. Each data point is the average of duplicate assays.

Figure 3-5

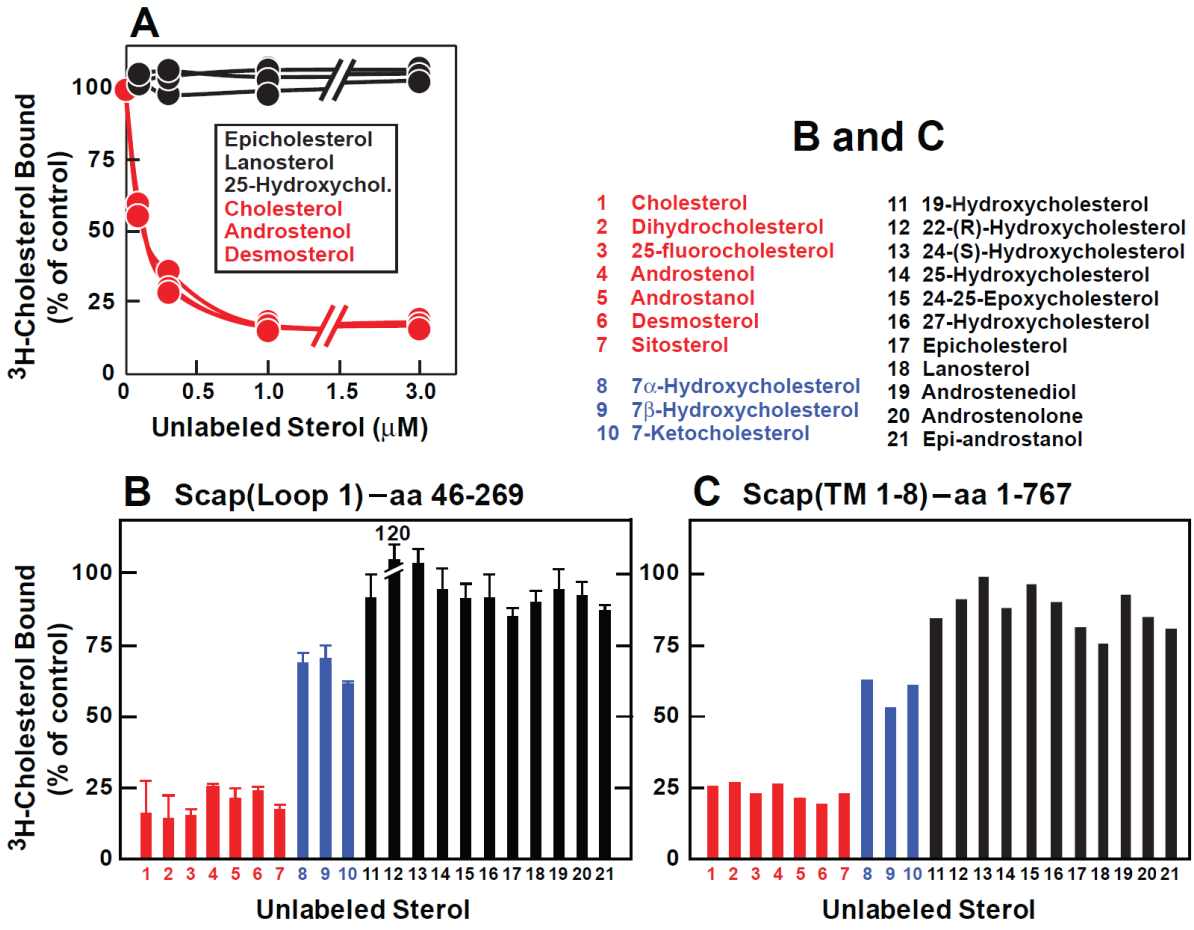
A
100
75
50
25
0
0
0.5
1.0
1.5
3.0
3H-Cholesterol Bound (% of control)
Unlabeled Sterol (μM)
Epicholesterol
Lanosterol
25-Hydroxychol.
Cholesterol
Androstenol
Desmosterol
B and C
1 Cholesterol
2 Dihydrocholesterol
3 25-fluorocholesterol
4 Androstenol
5 Androstanol
6 Desmosterol
7 Sitosterol
8 7α-Hydroxycholesterol
9 7β-Hydroxycholesterol
10 7-Ketocholesterol
11 19-Hydroxycholesterol
12 22-(R)-Hydroxycholesterol
13 24-(S)-Hydroxycholesterol
14 25-Hydroxycholesterol
15 24-25-Epoxycholesterol
16 27-Hydroxycholesterol
17 Epicholesterol
18 Lanosterol
19 Androstenediol
20 Androstenolone
21 Epi-androstanol
B Scap(Loop 1)−aa 46-269
C Scap(TM 1-8)−aa 1-767
120
100
75
50
25
0
1 2 3 4 5 6 7 8 9 10 11 12 13 14 15 16 17 18 19 20 21
3H-Cholesterol Bound (% of control)
Unlabeled Sterol
Unlabeled Sterol

FIGURE 3-6. Alanine scan mutagenesis of Loop 1 region of hamster Scap.

A, B, on day 0, SRD-13 cells were set up for experiments in 1 ml of medium A containing 5% FCS at a density of $3x10^4$ cells per well in 24-well plates. On day 1, cells in 1 ml of medium A supplemented with 5% FCS were cotransfected with 38 ng of pTK-Insig1-Myc, 125 ng pSRE-Firefly-Luciferase, 125 ng of pTK-*Renilla* luciferase, and 50 ng of WT pTK-Scap or the indicated mutant pTK-Scap in which 1 to 3 residues were mutated to alanine. FuGENE 6 was used as the transfection agent. For each transfection, the total amount of DNA was adjusted to 338 ng/dish by addition of pDNA3 mock vector. On day 2 (after incubation with plasmids for 24 h), the cells were washed once with PBS and then treated with hydroxypropyl-β-cyclodextrin-containing medium B for 1 h. Cells were then washed twice with PBS and refed with 1 ml of medium C in the absence or presence of 15 μM cholesterol complexed with methyl-β-cyclodextrin. After incubation for 16 h, the cells were washed with PBS, after which luciferase activity was read on a Synergy 4 plate reader (BioTek) according to the Promega protocol. The amount of SRE-firefly luciferase activity in each dish was normalized to the amount of *Renilla* luciferase activity in the same dish. "Relative SRE-luciferase Activity" of 1.0 represents the normalized luciferase value in dishes transfected with WT pTK-Scap in the absence of cholesterol. All values are the average of duplicate assays. *A,* red asterisks denote single, double, or triple contiguous alanine mutations that produced a loss of SRE-luciferase activity in both the absence and presence of cholesterol. The data in these graphs were obtained in 4 different experiments, each with its own WT control. *B,* deconvolution of double or triple mutants that showed loss of SRE-luciferase activity in *A.* Red boxes denote single alanine mutations that continued to show loss of SRE-luciferase activity. Each value is the average of duplicate assays.

Figure 3-6

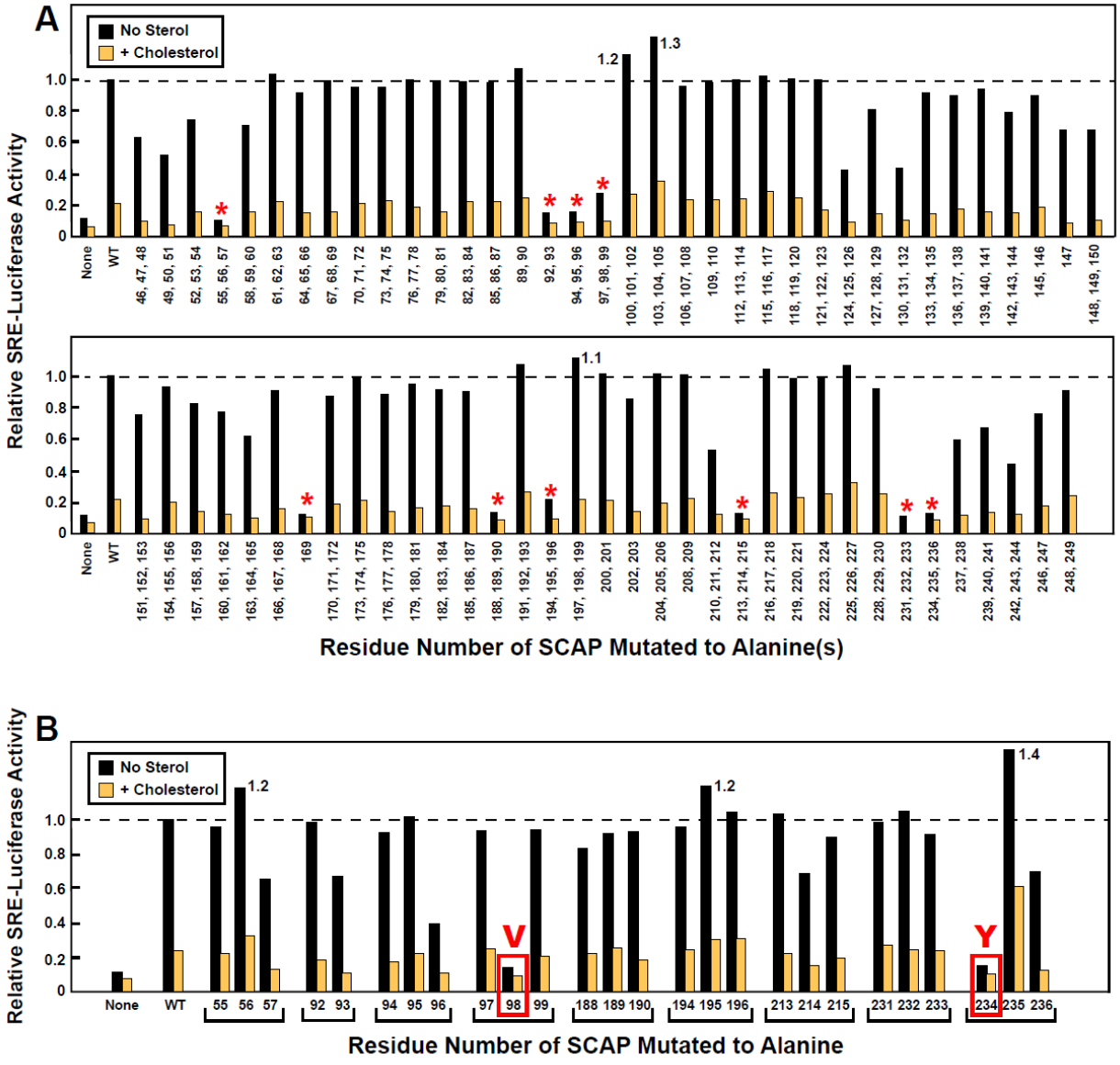
A
No Sterol
+ Cholesterol
Relative SRE-Luciferase Activity
1.2
1.3
1.1
Residue Number of SCAP Mutated to Alanine(s)
B
No Sterol
+ Cholesterol
Relative SRE-Luciferase Activity
1.2
1.2
1.4
V
Y
None
WT
55 56 57
92 93
94 95 96
97 98 99
188 189 190
194 195 196
213 214 215
231 232 233
234 235 236
Residue Number of SCAP Mutated to Alanine

FIGURE 3-7. ER-to-Golgi transport of WT and Y234A mutant version of GFP-Scap.

On day 0, SV589 cells were set up for experiments in medium D at a density of $1x10^5$ cells per 37-mm dish containing three 12-mm glass coverslips. On day 1, cells were transfected with 1 μg of full length WT pGFP-Scap (*top panels*) or its mutant Y234A version (*bottom panels*) in 3 ml of medium A supplemented with 5% FCS. FuGENE 6 was used as the transfection reagent. On day 2, the cells were washed once with PBS and then incubated for 1 h at 37°C with cyclodextrin-containing medium B supplemented with 50 μg/ml cycloheximide, after which each coverslip was fixed, permeabilized in methanol at -20°C for 15 min, and then incubated with 0.625 μg/ml of a monoclonal antibody against the Golgi resident protein GM130 (BD Biosciences) followed by 6.7 μg/ml of goat anti-mouse antibodies conjugated to Alexa 594 (Invitrogen). The nuclei were then stained with 1 μg/ml Hoechst 33342 (Invitrogen), and the coverslips were mounted in Mowiol 4-88 (Calbiochem) mounting solution (Wei and Seemann, 2009). Fluorescence images were acquired using an LD Plan-Neofluar 40x/1.3 DIC objective, an Axiovert 200M microscope (Zeiss), an Orca 285 camera (Hamamatsu) and the software Openlab 4.0.2 (Improvision). Scale bar, 10 μm.

Figure 3-7

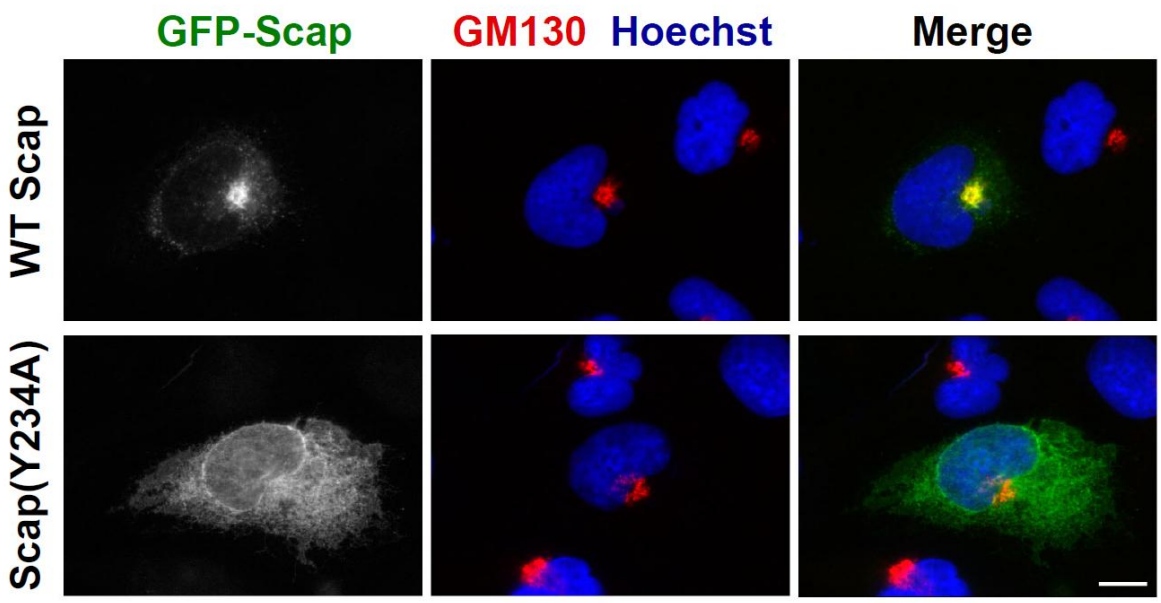

FIGURE 3-8. Biochemical characterization of the Y234A mutant Scap.

A, Immunoblot analysis of SREBP-2 in Scap-deficient cells transfected with WT or Y234A mutant version of full length Scap in the absence or presence of transfected Insig-1. On day 0, SRD-13A cells were set up for experiments at a density of $3x10^5$ cells per 60-mm dish in 4 ml of medium A containing 5% FCS. On day 2, cells were transfected with 2 μg TK-HSV-BP2 and 0.4 μg of full length pTK-Scap (WT or its Y234A mutant) with or without 0.3 μg of pTK-Insig 1-Myc in 7 ml of medium A supplemented with 5% FCS; FuGENE 6 was used as the transfection agent. For each transfection, the total amount of DNA was adjusted to 2.7 μg/dish by addition of pDNA3 mock vector. On day 3, cells were washed once with PBS and then switched to hydroxypropyl-β-cyclodextrin-containing medium B for 1 h. The cells were washed with PBS and then incubated with medium C containing either 30 μM cholesterol complexed with methyl-β-cyclodextrin or 1 μg/ml 25-hydroxycholesterol (delivered in ethanol, final concentration of 0.1%) as indicated. After incubation for 4 h, the cells were harvested, and the isolated nuclear and membrane fractions were subjected to immunoblot analysis with 0.2 μg/ml anti-HSV (SREBP-2), 5 μg/ml IgG-4H4 (Scap), or 1 μg/ml anti-Myc IgG-9E10 (Insig). Films were exposed for 8 to 20 sec. *B*, [^{3}H]cholesterol binding to WT and Y234A mutant version of His_6-Scap(Loop1). Each reaction, in a final volume of 100 μl buffer C with 0.004% NP-40 and 0.001% Fos-choline 13, contained 5 pmol of purified WT and Y234A mutant version of His_6-Scap(Loop1), 1 μg bovine serum albumin, and the indicated concentration of [^{3}H]cholesterol ($222x10^3$ dpm/pmol) in the absence or presence of 10 μM unlabeled cholesterol. After 4 h at room temperature, the bound [^{3}H]cholesterol was measured as described in *Experimental Procedures*. Each data point is the average of duplicate assays and represents specific binding after subtraction of blank values determined in the presence of unlabeled cholesterol. *C*, tryptic

digestion of WT and Y234A mutant version of full length Scap transfected into Scap-deficient hamster cells. SRD-13A cells were transfected with the indicated full length pCMV-Scap plasmid and harvested for preparation of membranes as described in *Experimental Procedures*. Aliquots of the 20,000x*g* membrane fractions (100 μg) were incubated for 20 min at room temperature with 50 μM cholesterol complexed with methyl-β-cyclodextrin, followed by sequential treatments with 14 μg/ml trypsin (30 min at 30°C) and 4000 U/ml PNGase F (4 h at 37°C). The samples were then subjected to immunoblot analysis with 5 μg/ml anti-Scap IgG-4H4. The film was exposed for 30 sec. *D*, immune detection of Scap•Insig-1 complexes. On day 2, SRD-13A cells were cotransfected with pCMV-Insig1-Myc together with either full length pCMV-Scap or its mutant Y234A version as indicated. On day 3, the cells were incubated for 1 h with 1% hydroxypropyl-β-cyclodextrin, after which they received fresh medium containing one of the following sterols: none (-), 30 μM cholesterol complexed with methyl-β-cyclodextrin (Chol), or 1 μg/ml 25-HC. After incubation at 37°C for 4 h, each detergent-solubilized whole cell lysate was incubated with anti-Myc beads, followed by washing and elution with Myc peptide as described in *Experimental Procedures*. The eluates were subjected to immunoblot analysis with either 5 μg/ml anti-Scap IgG-4H4 or 1 μg/ml anti-Myc IgG-9E10. Films were exposed for 3-5 sec.

Figure 3-8

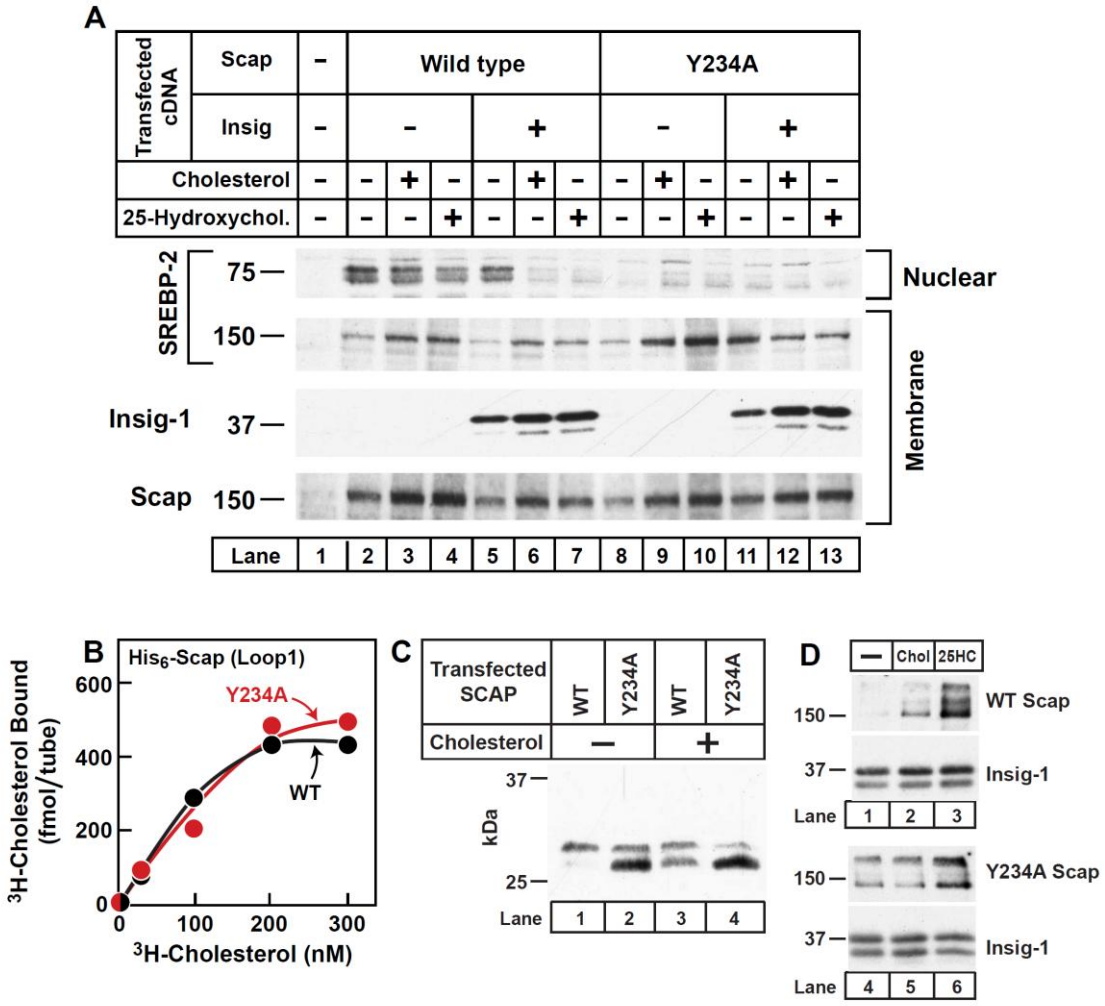
A
Transfected cDNA
Scap
Insig
Wild type
Y234A
Cholesterol
25-Hydroxychol.
SREBP-2
75
150
Nuclear
Membrane
Insig-1
37
Scap
150
Lane
1 2 3 4 5 6 7 8 9 10 11 12 13
B
His6-Scap (Loop1)
Y234A
WT
3H-Cholesterol Bound (fmol/tube)
3H-Cholesterol (nM)
0 100 200 300
0 200 400 600
C
Transfected SCAP
WT
Y234A
WT
Y234A
Cholesterol
kDa
37
25
Lane
1 2 3 4
D
Chol
25HC
150
WT Scap
37
Insig-1
Lane
1 2 3
150
Y234A Scap
37
Insig-1
Lane
4 5 6

FIGURE 3-9. Cycloheximide-mediated decline in transfected WT and Y234A mutant version of GFP-Scap in CHO cells.

On day 0, CHO-K1 cells were set up for experiments in 10 ml of medium A containing 5% FCS at a density of $6x10^5$ cells per 100-mm dish. On day 2, cells were transfected with 1 μg of WT GFP-Scap or its Y239A mutant version in 7 ml of medium A supplemented with 5% FCS. FuGENE 6 was used as the transfection agent. On day 3, cells were switched to 7 ml of medium A supplemented with 5% FCS containing 50 μM cycloheximide. At the indicated time after addition of cycloheximide, cells were washed once with PBS and then solubilized with buffer containing 1% (w/v) SDS, 10 mM Tris-HC1 (pH 7.4), and 100 mM NaCl. The detergent solubilized lysate was subjected to immunoblot analysis with 1 μg/ml anti-GFP. Film was exposed for 6 sec (*Inset*). The level of GFP-Scap protein was quantified by J. Image and plotted.

Figure 3-9

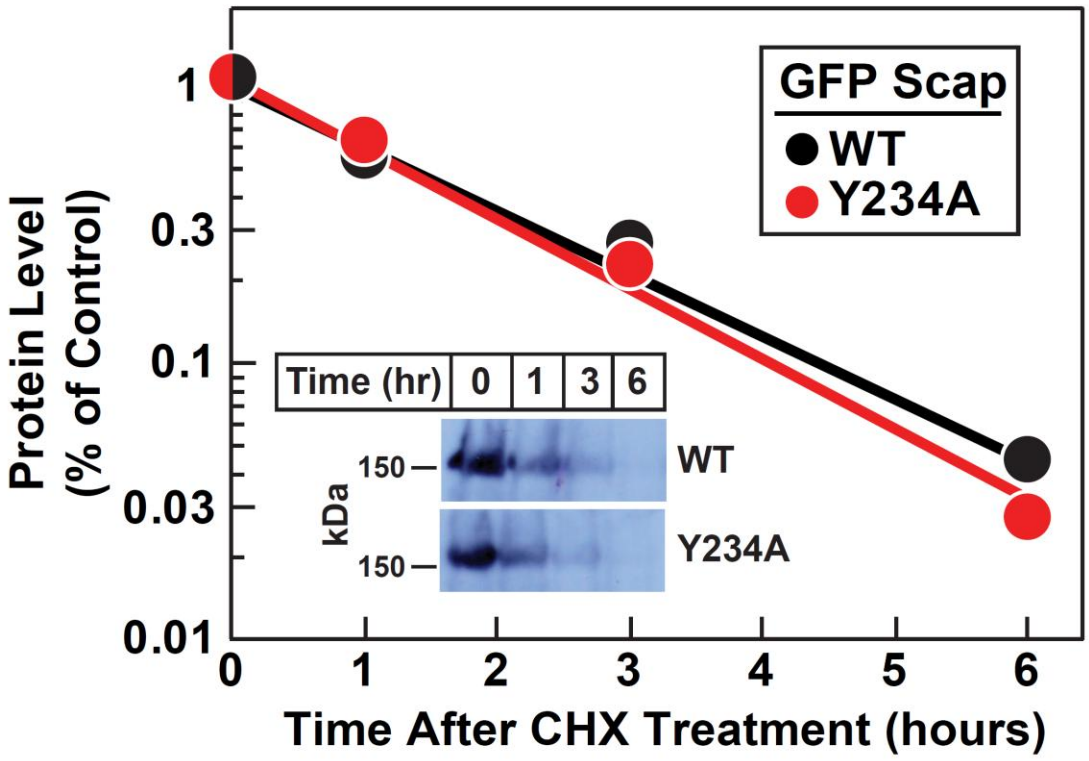

DISCUSSION

The studies in this paper identify Loop 1 of Scap as a crucial component of the cholesterol-sensing mechanism in animal cells. When examined *in vitro*, this loop binds sterols with specificity that is identical to that of the whole membrane attachment domain (TM1-8). Moreover, a single point mutation in Loop 1 (Y234A) converts Loop 6 of Scap constitutively into the cholesterol-bound conformation as monitored by the protease protection assay. Consistent with this observation, Scap(Y234A) binds to Insig even in sterol-depleted cells, and it cannot transport SREBP-2 to the Golgi, even after sterol depletion. These findings are consistent with the protease protection assay and suggest that the MELADL sequence in Scap(Y234A) is unable to interact with COPll proteins. Precisely how a change in Loop 1 causes a change in Loop 6 is not known, but the current findings establish this interplay as a crucial element in the regulation of cholesterol metabolism in animal cells.

The way in which a luminal loop of Scap binds intramembrane cholesterol remains to be determined. When expressed in insect cells, this loop is bound tightly to membranes, most likely ER membranes. The protein cannot be released by chaotropic agents, and it requires detergents for extraction. Loop 1 contains three hydrophobic segments, as indicated in yellow in Fig. 3-1. None of these has the characteristics of a membrane-spanning helix as determined by hydrophobicity plots (see Fig. 1 of Nohturfft, *et al.*) (Nohturfft et al., 1998). The evidence that Loop 1 lies in the ER lumen is based on studies of the glycosylation site at amino acid 263 in this loop (Fig. 3-1). This sequence was shown to be glycosylated when full-length Scap was produced in CHO cells (Nohturfft et al., 1998). It seems likely that the hydrophobic segments in Loop 1 dip into the membrane, but do not cross it. Within the membrane, these segments would be in a position to bind intramembrane cholesterol.

Our alanine scanning mutagenesis failed to identify residues that are crucial for cholesterol binding, as indicated by the SRE-luciferase reporter assay (Fig. 3-6). It is possible that crucial cholesterol-binding residues could be identified by substituting amino acids other than alanine. Definitive identification of the cholesterol-binding site would be revealed if the structure of the loop could be studied by X-ray crystallography. Studies along these lines are under way.

In our [^{3}H]cholesterol-binding assays with recombinant Scap(Loop1), we used detergent concentrations that are at the borderline for micelle formation (0.004% NP-40 plus 0.001% Fos-choline-13). Moreover, we washed the nickel column and eluted the protein with solutions that lacked detergent. These conditions were determined empirically to produce an optimal ratio of specific to nonspecific [^{3}H]cholesterol binding. Under these conditions, we estimated that at saturation, 1 mole of [^{3}H]cholesterol bound to 4-5 moles of Scap(Loop1). Inasmuch as Scap(Loop1) behaved at a tetramer by gel filtration, the binding stoichiometry raises the possibility that one mole of tetramer binds one mole of cholesterol. In experiments not shown, we subjected cholesterol-bound Loop 1 to gel filtration, and the protein continued to behave as a tetramer. We therefore believe that cholesterol binding does not alter the tetrameric state. We have no data as to the oligomerization state of Scap in ER membranes. Such studies are currently in progress.

Inasmuch as a crucial residue is a tyrosine at position 234, we considered the possibility that the hydroxyl group must be phosphorylated or otherwise modified in order for Scap to exit the ER. This possibility was excluded when we substituted phenylalanine for tyrosine-234 in full length Scap and found that this protein reached the Golgi normally (data not shown).

We also considered the formal possibility that Scap(Y234A) was simply failing to fold properly and was retained in the ER through the unfolded protein response. Several observations argued strongly against this possibility: 1) Scap(Y234A) showed the appropriate cleavage patterns for the cholesterol-bound configuration when treated with trypsin (Fig. 3-8C); 2) Scap(Y234A) bound to Insig-1 (Fig.3-8D); and 3) Scap(Y234A) and WT Scap had similar half-lives as revealed by the rate of decline of the proteins after protein synthesis was inhibited with cycloheximide (Fig. 3-9). If Scap(Y234A) were misfolded, it would be expected to be degraded more rapidly.

In earlier papers, we referred to the region of Scap containing transmembrane helices 2-6 as the "sterol-sensing domain" (Hua et al., 1996; Nohturfft et al., 1998). This nomenclature was based on the observation that evolutionarily related sequences are present in other membrane proteins that are postulated to interact with or be influenced by sterols. The other proteins include HMG CoA reductase, an ER-bound enzyme whose degradation is accelerated by sterols (Gil et al., 1985; Skalnik et al., 1988); NPC1, a protein involved in the transport of cholesterol from lysosomes to the ER and to the plasma membrane (Pentchev et al., 1995); and patched, which is the receptor for hedgehog, the only protein known to contain covalently-bound cholesterol (Porter et al., 1996). In view of the current data showing that the cholesterol-binding site in Scap is located in Loop 1 and previous data showing that the TM 2-6 segment of Scap is the Insig-binding domain (Yang et al., 2002; Yabe et al., 2002a), we will henceforth refer to the TM 2-6 segment as the Insig-binding domain (Fig. 3-1). We have not ruled out the possibility that the Insig-binding domain contains another sterol-binding site. We think this possibility is unlikely because our previous study of sterol binding to the entire TM 1-8 region of Scap showed evidence of only a single class of binding sites, and this class has the same properties as the

binding site in Loop 1. It is noteworthy that the corresponding TM 2-6 segment of HMG CoA reductase binds to Insig in a sterol-dependent fashion (Sever et al., 2003). The roles of the corresponding transmembrane segment in NPC1 and patched remain to be determined. However, recent biochemical and crystallographic studies showed that the initial sterol-binding site in NPC1 is not contained in the transmembrane segment, but rather it lies in the N-terminal domain of the protein, which, like Loop 1 of Scap, projects into the lumen of the ER (Infante et al., 2008a; Kwon et al., 2009).

The current studies add important insights into the mechanisms by which a membrane protein monitors the levels of cholesterol in cell membranes.

Material from Chapter 3 was originally published in Journal of Biological Chemistry. Motamed M, Zhang Y, Wang ML, Seemann J, Kwon HJ, Goldstein JL, Brown MS. Identification of Luminal Loop 1 of Scap as the Sterol Sensor that Maintains Cholesterol Homeostasis. *J Biol Chem.* 2010 May 20;286(20):18002-12.

CHAPTER 4

CONCLUSION AND PERSEPECTIVE

Cholesterol homeostasis has implications in disease, which accounts for the strict regulation of cholesterol import and synthesis. Cholesterol import begins at LDL uptake via the LDL receptor. After receptor-mediated endocytosis, LDL particles are transported to the lysosomes, where they are degraded, and cholesteryl esters are released. Acid lipase then cleaves cholesteryl esters, releasing cholesterol in the early endosomes. Through the sequential action of NPC2 and NPC1, cholesterol is exported from the lysosomes (Kwon et al., 2009). From there, cholesterol travels to the ER where it exerts its regulatory role, including a feedback mechanism for further synthesis.

This thesis has focused on understanding the biochemical basis for sterol sensing, through a study of the proteins involved in sterol transfer and recognition. An initial and more rigorous understanding of proteins involved in cholesterol transport can be gained by considering NPC2 and NPC1, as crystal structures of the binding domains of both proteins have been solved. Further, cholesterol recognition can be further analyzed by considering our study of Scap, where its cholesterol recognition function controls the feedback mechanisms underlying cholesterol homeostasis. Finally, a synthesis of our studies can be used to draw conclusions about how proteins bind cholesterol.

Prior to our studies of NPC2, the structures of cholesterol-binding proteins NPC2 and NPC1(NTD) had been solved. They are similar in that the cholesterol is surrounded by a distinct binding pocket (Xu et al., 2007 and Kwon et al., 2009). This pocket hides the hydrophobic, tetracyclic structure of cholesterol from solvent and surrounds the molecule by an

overrepresentation of hydrophobic amino acids including phenylalanine and isoleucine. Further supporting their roles as carriers of cholesterol, rather than enzymes that modify sterols is the observation that the apo and cholesterol-bound forms of the proteins are nearly identical.

In contrast to the similar nature of the binding pockets, the NPC proteins as a whole are distinct: NPC2 is a small soluble protein, while NPC1 is a 1278 amino acid lysosomal membrane-bound protein. This difference helps to elucidate the relationship between NPC1 and NPC2, which provides great insight, as it highlights the necessity of maintaining insoluble cholesterol in solution. The function of NPC2 is strictly to counteract the potential precipitation and crystallization of cholesterol, ensuring that free cholesterol is available in the lysosome and delivered to NPC1, which is immobilized by its membrane attachment. The delivery of cholesterol to NPC1 is at its NTD, a portion of the protein tethered in the lysosomal lumen (Infante et al., 2008b).

The importance of NPC1 being membrane bound is better appreciated when looking beyond the initial step of cholesterol binding. After the NTD, NPC1 contains a proline-rich-region, which may enable NPC1 to move cholesterol, so that it may export from the lysosome (Kwon et al., 2009). This proline-rich-region would behave as a hinge upon which the NTD can deliver cholesterol into a sort of cholesterol pore in the lysosomal membrane. This linker region would be of importance in allowing NPC1 to function not only as the cholesterol acceptor protein of the lysosome, but additionally as the cholesterol exporter.

Our current understanding is that NPC2 presents cholesterol to NPC1(NTD). We have created this model by evaluating our current data. This analysis includes site-directed mutagenesis studies providing transfer mutants for NPC1(NTD) and NPC2 and kinetic data

demonstrating that NPC2 accelerates NPC1(NTD) cholesterol binding. However, we have yet to demonstrate a physical interaction between the two proteins. Our efforts have included gel-filtration, co-immunoprecipitation, affinity chromatography, AlphaScreen, surface plasmon resonance, and cross-linking. Presumably, the transient nature of the interaction has precluded a direct identification of the NPC2:NPC1(NTD) complex. If so, considering a dynamic assay sensitive to changes on the millisecond time scale such as NMR, as opposed to an end-point assay, might be beneficial.

Once the cholesterol is exported from the lysosome, it enters the ER where it exerts a regulatory role. Scap is the sensor of ER cholesterol, and when cholesterol levels are high, it prevents release of SREBP, a transcription factor that increases transcription of enzymes associated with cholesterol synthesis. In our study, we identify the first luminal loop of Scap as the cholesterol sensor. Scap appears to be another specific instance of cholesterol binding to a luminal domain.

When membrane cholesterol content is around 4% or lower, SREBP is released, allowing for increased expression of genes associated with cholesterol synthesis (Radhakrishnan et al., 2008). However when cholesterol content is exceeds 6%, SREBP is retained, limiting expression of genes associated with cholesterol synthesis (Radhakrishnan et al., 2008). The localization of Scap's cholesterol binding pocket to a luminal loop might seem appropriate considering that a 2% differential in membrane cholesterol content provides a drammatic effect regarding the regulation of the Scap-SREBP interaction. Alternatively, past some threshold of ER cholesterol content, cholesterol might become exposed from the membrane, allowing for greater thermodynamic regulation of Scap's cholesterol binding.

Scap also has a cholesterol-responsive capacity. In our studies, we indentified Scap mutation Y234A. This mutant Scap binds cholesterol with normal thermodynamics, but the unliganded protein maintains a cholesterol-bound conformation, as monitored by a readout involving Loop 7. This result demonstrates that the Loop 1 of Scap is capable of relaying the signal of cholesterol binding to other parts of the protein, which may then have a funtional response. This response includes movement of Loop 6, masking the MELADL sequnce in the case of the Y234 mutant. This movement of MELADL then precludes COP II binding to Scap and therefore SREBP release.

Our studies of NPC1 and Scap can lend support to the generality that proteins bind sterols by means of a luminal domain. Cholesterol homeostasis is tightly monitored, and the membrane composition of cholesterol varies little (Radhakrishnan et al., 2008). Therefore, it seems difficult to imagine that proteins would be able to recognize and respond to these subtle fluctuations in membrane-cholesterol content. Instead, cholesterol's association with the membrane may change past some membrane-cholesterol threshold. If cholesterol becomes exposed at the periphery of the membrane, the luminal domain of a protein can then have access to this cholesterol and respond appropriately.

The improtance of cholesterol homeostasis has been well understood for many years. In contrast, a true biochemical understanding of how cholesterol-binding and responsive proteins recognize subtle differences in membrane-cholesterol content has yet to be fully understood. Our biochemical studies of Scap and NPC proteins might provide an insight that cholesterol recognition is not deep in the membrane, but somehow in its periphery.

This analysis is complicated by the fact the Scap's first loop appears as a membrane bound protein when expressed in insect cells. This binding is attributed to three hydrophobic patches contained within the loop (Fig. 3-1). Therefore, the possibilty that these hydrophobic residues recognize cholesterol in the membrane cannot be totally excluded. To explore this possibilty further, our lab has undertaken the project of crystallizing this loop of Scap. A crystal structure would be of great utility because it would completely elucidate the physical means of cholesterol recognition by Scap.

Additionally, it would be informative to identify the protein involved in cholesterol export from the lysosome after NPC1(NTD) has bound the cholesterol. Once the NPC1 protein has bound cholesterol in the lumen of the lysosome, the cholesterol has to pass through the lysosomal bilayer. Perhaps this transfer is mediated by NPC1 or another protein. Either way, it seems probable that a protein-mediated movement is required. Isolating the next sequential protein involved should assist delineating that specific mechanism.

BIBLIOGRAPHY

Anderson, K.S. (1999). Fundamental mechanisms of substrate channeling. Methods Enzymol *308*, 111-145.

Babalola, J.O., Wendeler, M., Breiden, B., Arenz, C., Schwarzmann, G., Locatelli-Hoops, S., and Sandhoff, K. (2007). Development of an assay for the intermembrane transfer of cholesterol by Niemann-Pick C2 protein. Biol Chem *388*, 617-626.

Brown, A.J., Sun, L., Feramisco, J.D., Brown, M.S., and Goldstein, J.L. (2002). Cholesterol addition to ER membranes alters conformation of SCAP, the SREBP escort protein that regulates cholesterol metabolism. Mol. Cell *10*, 237-245

Brown, M.S., Faust, J.R., Goldstein, J.L., Kaneko, I., and Endo, A. (1978). Induction of 3-hydroxy-3-methylglutaryl coenzyme A reductase activity in human fibroblasts incubated with compactin (ML-236B), a competitive inhibitor of the reductase. J. Biol. Chem. *253*, 1121-1128.

Brown, M.S., and Goldstein, J.L. (1986). A receptor-mediated pathway for cholesterol homeostasis. Science *232*, 34-47.

Brown, M.S., and Goldstein, J.L. (1997). The SREBP pathway: regulation of cholesterol metabolism by proteolysis of a membrane-bound transcription factor. Cell *89*, 331-340.

Carstea, E.D., Morris, J.A., Coleman, K.G., Loftus, S.K., Zhang, D., Cummings, C., Gu, J., Rosenfeld, M.A., Pavan, W.J., Krizman, D.B., *et al.* (1997). Niemann-Pick C1 disease gene: homology to mediators of cholesterol homeostasis. Science *277*, 228-231.

Chang, T.Y., Chang, C.C., Ohgami, N., and Yamauchi, Y. (2006). Cholesterol sensing, trafficking, and esterification. Annu Rev Cell Dev Biol *22*, 129-157.

Chang, T.Y., Reid, P.C., Sugii, S., Ohgami, N., Cruz, J.C., and Chang, C.C. (2005). Niemann-Pick type C disease and intracellular cholesterol trafficking. J Biol Chem *280*, 20917-20920.

Chikh, K., Vey, S., Simonot, C., Vanier, M.T., and Millat, G. (2004). Niemann-Pick type C disease: importance of N-glycosylation sites for function and cellular location of the NPC2 protein. Mol Genet Metab *83*, 220-230.

Dahl, N.K., Reed, K.L., Daunais, M.A., Faust, J.R., and Liscum, L. (1992). Isolation and characterization of Chinese hamster ovary cells defective in the intracellular metabolism of low density lipoprotein-derived cholesterol. J Biol Chem *267*, 4889-4896.

Feramisco, J.D., Radhakrishnan, A., Ikeda, Y., Reitz, J., Brown, M.S., and Goldstein, J.L. (2005). Intramembrane aspartic acid in SCAP protein governs cholesterol-induced conformational change. Proc. Natl. Acad. Sci. USA *102*, 3242-3247.

Gil, G., Faust, J.R., Chin, D.J., Goldstein, J.L., and Brown, M.S. (1985). Membrane-bound domain of HMG CoA reductase is required for sterol-enhanced degradation of the enzyme. Cell *41*, 249-258.

Goldstein, J.L., Basu, S.K., and Brown, M.S. (1983). Receptor-mediated endocytosis of low-density lipoprotein in cultured cells. Methods Enzymol *98*, 241-260.

Goldstein, J.L., DeBose-Boyd, R.A., and Brown, M.S. (2006). Protein sensors for membrane sterols. Cell *124*, 35-46.

Gong, Y., Lee, J.N., Lee, P.C.W., Goldstein, J.L., Brown, M.S., and Ye, J. (2006). Sterol-regulated ubiquitination and degradation of Insig-1 creates a convergent mechanism for feedback control of cholesterol synthesis and uptake. Cell Metabolism *3*, 15-24.

Hannah, V.C., Ou, J., Luong, A., Goldstein, J.L., and Brown, M.S. (2001). Unsaturated fatty acids down-regulate SREBP isoforms 1a and 1c by two mechanisms in HEK-293 cells. J. Biol. Chem. *276*, 4365-4372.

Horton, J.D., Goldstein, J.L., and Brown, M.S. (2002). SREBPs: activators of the complete program of cholesterol and fatty acid synthesis in the liver. J. Clin. Invest. *109*, 1125-1131.

Hua, X., Nohturfft, A., Goldstein, J.L., and Brown, M.S. (1996). Sterol resistance in CHO cells traced to point mutation in SREBP cleavage-activating protein. Cell *87*, 415-426.

Ikeda, Y., DeMartino, G.N., Brown, M.S., Lee, J.N., Goldstein, J.L., and Ye, J. (2009). Regulated endoplasmic reticulum-associated degradation of a polytopic protein: p97 recruits proteasomes to Insig-1 before extraction from membranes. J. Biol. Chem. *284*, 34889-34900.

Infante, R.E., Abi-Mosleh, L., Radhakrishnan, A., Dale, J.D., Brown, M.S., and Goldstein, J.L. (2008a). Purified NPC1 protein. I. Binding of cholesterol and oxysterols to a 1278-amino acid membrane protein. J Biol Chem *283*, 1052-1063.

Infante, R.E., Radhakrishnan, A., Abi-Mosleh, L., Kinch, L.N., Wang, M.L., Grishin, N.V., Goldstein, J.L., and Brown, M.S. (2008b). Purified NPC1 protein: II. Localization of sterol binding to a 240-amino acid soluble luminal loop. J Biol Chem *283*, 1064-1075.

Infante, R.E., Wang, M.L., Radhakrishnan, A., Kwon, H.J., Brown, M.S., and Goldstein, J.L. (2008c). NPC2 facilitates bidirectional transfer of cholesterol between NPC1 and lipid bilayers, a step in cholesterol egress from lysosomes. Proc Natl Acad Sci U S A *105*, 15287-15292.

James, C.L., and Viola, R.E. (2002). Production and characterization of bifunctional enzymes. Substrate channeling in the aspartate pathway. Biochemistry *41*, 3726-3731.

Kapust, R.B., Tozser, J., Copeland, T.D., and Waugh, D.S. (2002). The P1' specificity of tobacco etch virus protease. Biochem. Biophys. Res. Comm. *294*, 949-955.

Kita, T., Brown, M.S., and Goldstein, J.L. (1980). Feedback regulation of 3-hydroxy-3-methylglutaryl coenzyme A reductase in livers of mice treated with mevinolin, a competitive inhibitor of the reductase. J. Clin. Invest. *66*, 1094-1100.

Ko, D.C., Binkley, J., Sidow, A., and Scott, M.P. (2003). The integrity of a cholesterol-binding pocket in Niemann-Pick C2 protein is necessary to control lysosome cholesterol levels. Proc Natl Acad Sci U S A *100*, 2518-2525.

Kornfeld, S. (1987). Trafficking of lysosomal enzymes. FASEB J *1*, 462-468.

Kwon, H.J., Abi-Mosleh, L., Wang, M.L., Deisenhofer, J., Goldstein, J.L., Brown, M.S., and Infante, R.E. (2009). Structure of N-terminal domain of NPC1 reveals distinct subdomains for binding and transfer of cholesterol. Cell *137*, 1213-1224.

Loftus, S.K., Morris, J.A., Carstea, E.D., Gu, J.Z., Cummings, C., Brown, A., Ellison, J., Ohno, K., Rosenfeld, M.A., Tagle, D.A., *et al.* (1997). Murine model of Niemann-Pick C disease: mutation in a cholesterol homeostasis gene. Science *277*, 232-235.

Motamed, M., Zhang, Y., Wang, M.L., Seemann, J., Kwon, H.J., Goldstein, J.L., and Brown, M.S. (2011). Identification of luminal loop 1 of Scap as the sterol sensor that maintains cholesterol homeostasis. J Biol Chem *286*, 18002-18012.

Naureckiene, S., Sleat, D.E., Lackland, H., Fensom, A., Vanier, M.T., Wattiaux, R., Jadot, M., and Lobel, P. (2000). Identification of HE1 as the second gene of Niemann-Pick C disease. Science *290*, 2298-2301.

Nohturfft, A., Brown, M.S., and Goldstein, J.L. (1998). Topology of SREBP Cleavage-activating Protein, a Polytopic Membrane Protein with a Sterol-sensing Domain. J Biol Chem *273*, 17243-17250.

Nohturfft, A., Yabe, D., Goldstein, J.L., Brown, M.S., and Espenshade, P.J. (2000). Regulated step in cholesterol feedback localized to budding of SCAP from ER membranes. Cell *102*, 315-323.

Pentchev, P.G., Vanier, M.T., Suzuki, K., and Patterson, M.C. (1995). The Metabolic and Molecular Basis of Inherited Disease (New York, McGraw-Hill Inc.).

Porter, J.A., Young, K.E., and Beachy, P.A. (1996). Cholesterol modification of hedgehog signaling proteins in animal development. Science *274*, 255-259.

Radhakrishnan, A., Goldstein, J.L., McDonald, J.G., and Brown, M.S. (2008). Switch-like control of SREBP-2 transport triggered by small changes in ER cholesterol: a delicate balance. Cell Metab *8*, 512-521.

Radhakrishnan, A., Ikeda, Y., Kwon, H.J., Brown, M.S., and Goldstein, J.L. (2007). Sterol-regulated transport of SREBPs from endoplasmic reticulum to Golgi: oxysterols block transport by binding to Insig. Proc Natl Acad Sci U S A *104*, 6511-6518.

Radhakrishnan, A., Sun, L., Kwon, H.J., Brown, M.S., and Goldstein, J.L. (2004). Direct Binding of Cholesterol to the Purified Membrane Region of SCAP: Mechanism for a Sterol-Sensing Domain. Mol Cell *15*, 259-268.

Rawson, R.B., DeBose-Boyd, R., Goldstein, J.L., and Brown, M.S. (1999). Failure to cleave sterol regulatory element-binding proteins (SREBPs) causes cholesterol auxotrophy in Chinese hamster ovary cells with genetic absence of SREBP cleavage-activating protein. J Biol Chem *274*, 28549-28556.

Sakai, J., Nohturfft, A., Cheng, D., Ho, Y.K., Brown, M.S., and Goldstein, J.L. (1997). Identification of complexes between the COOH-terminal domains of sterol regulatory element binding proteins (SREBPs) and SREBP cleavage-activating protein (SCAP). J. Biol. Chem. *272*, 20213-20221.

Sever, N., Song, B.-L., Yabe, D., Goldstein, J.L., Brown, M.S., and DeBose-Boyd, R.A. (2003). Insig-dependent ubiquitination and degradation of mammalian 3-hydroxy-3-methylglutaryl CoA reductase stimulated by sterols and geranylgeraniol. J. Biol. Chem. *278*, 52479-52490.

Skalnik, D.G., Narita, H., Kent, C., and Simoni, R.D. (1988). The membrane domain of 3 hydroxy-3-methylglutaryl-coenzyme A reductase confers endoplasmic reticulum localization and sterol-regulated degradation onto beta-galactosidase. J. Biol. Chem. *263*, 6836-6841.

Smith, P.K., Krohn, R.I., Hermanson, G.T., Mallia, A.K., Gartner, F.H., Provenzano, M.D., Fujimoto, E.K., Goeke, N.M., Olson, B.J., and Klenk, D.C. (1985). Measurement of protein using bicinchoninic acid. Anal Biochem *150*, 76-85.

Sun, L.-P., Li, L., Goldstein, J.L., and Brown, M.S. (2005). Insig required for sterol-mediated inhibition of Scap/SREBP binding to COPII proteins *in vitro*. J. Biol. Chem. *280*, 26483-26490.

Sun, L.-P., Seemann, J., Brown, M.S., and Goldstein, J.L. (2007). Sterol-regulated transport of SREBPs from endoplasmic reticulum to Golgi: Insig renders sorting signal in Scap inaccessible to COPII proteins. Proc. Natl. Acad. Sci. USA *104*, 6519-6526.

Tessier, D.C., Thomas, D.Y., Khouri, H.E., Laliberte, F., and Vernet, T. (1991). Enhanced secretion from insect cells of a foreign protein fused to the honeybee melittin signal peptide. Gene *98*, 177-183.

Vanier, M.T., and Millat, G. (2003). Niemann-Pick disease type C. Clin Genet *64*, 269-281.

Verot, L., Chikh, K., Freydiere, E., Honore, R., Vanier, M.T., and Millat, G. (2007). Niemann-Pick C disease: functional characterization of three NPC2 mutations and clinical and molecular update on patients with NPC2. Clin Genet *71*, 320-330.

Wang, M.L., Motamed, M., Infante, R.E., Abi-Mosleh, L., Kwon, H.J., Brown, M.S., and Goldstein, J.L. (2010). Identification of surface residues on niemann-pick C2 essential for hydrophobic Handoff of cholesterol to NPC1 in lysosomes. Cell Metab *12*, 166-173.

Wei, J.-H. and Seemann, J. (2009). Induction of asymmetrical cell division to analyze spindle-dependent organelle partitioning using correlative microscopy techniques. Nature Protocols *4*, 1653-1662.

Yabe, D., Brown, M.S., and Goldstein, J.L. (2002a). Insig-2, a second endoplasmic reticulum protein that binds SCAP and blocks export of sterol regulatory element-binding proteins. Proc. Natl. Acad. Sci. USA *99*, 12753-12758.

Yabe, D., Xia, Z.-P., Adams, C.M., and Rawson, R.B. (2002b). Three mutations in sterol-sensing domain of SCAP block interaction with Insig and render SREBP cleavage insensitive to sterols. Proc. Natl. Acad. Sci. USA *99*, 16672-16677.

Yamamoto, T., Davis, C.G., Brown, M.S., Schneider, W.J., Casey, M.L., Goldstein, J.L., and Russell, D.W. (1984). The human LDL receptor: A cysteine-rich protein with multiple Alu sequences in its mRNA. Cell *39*, 27-38.

Yang, T., Espenshade, P.J., Wright, M.E., Yabe, D., Gong, Y., Aebersold, R., Goldstein, J.L., and Brown, M.S. (2002). Crucial step in cholesterol homeostasis: sterols promote binding of SCAP to INSIG-1, a membrane protein that facilitates retention of SREBPs in ER. Cell *110*, 489-500.

Xu, S., Benoff, B., Liou, H.L., Lobel, P., and Stock, A.M. (2007). Structural basis of sterol binding by NPC2, a lysosomal protein deficient in Niemann-Pick type C2 disease. J Biol Chem *282*, 23525-23531.